PREPARATION AND CHARACTERIZATION OF COCONUT SHELL DERIVED ACTIVATED CARBON FOR SUPERCAPACITOR APPLICATION

A DISSERTATION SUBMITTED TO THE

DEPARTMENT OF CHEMISTRY

AMRIT CAMPUS

INSTITUTE OF SCIENCE AND TECHNOLOGY

TRIBHUVAN UNIVERSITY

NEPAL

FOR THE PARTIAL FULFILLMENT OF REQUIREMENT OF THE MASTER OF SCIENCE DEGREE IN CHEMISTRY

BY

SARMILA DANGI

SYMBOL NO: 2180/077

T. U. REGD. NO.: 5-2-214-34-2016

MAY, 2024

BOARD OF EXAMINERS AND CERTIFICATE OF APPROVAL

The dissertation entitled **"PREPARATION AND CHARACTERIZATION OF COCONUT SHELL DERIVED ACTIVATED CARBON FOR SUPERCAPACITOR APPLICATION"** by **Ms. Sarmila Dangi** under the supervision of under the supervision of **Prof. Dr. Armila Rajbhandari (Nyachhyon)**, Department of Chemistry, Central Department, Tribhuvan University, Kathmandu, Nepal, and under the co-supervision of **Mr. Naresh Prashad Pant**, Department of Chemistry, Amrit Campus, Tribhuvan University, Kathmandu, Nepal, hereby submitted has been approved for partial fulfillment of the requirement for completion of her Master of Science (M.Sc.) Degree in Chemistry. This dissertation has not been submitted to any other university or institution previously for the award of a degree.

Tribhuvan University
Amrit Campus
Department of Chemistry

.....

Supervisor

Prof. Dr. Armila Rajbhandari

Central Department of Chemistry

Tribhuvan University

Kathmandu, Nepal

.....

Co-supervisor

Mr. Naresh Prashad Pant

Department of Chemistry

Amrit Campus, TU

Kathmandu, Nepal

.....

Internal Examiner

Assoc. Prof. Dr. Sharmila Pradhan

Department of Chemistry, Amrit Campus

TU, Kathmandu, Nepal

.....

External Examiner

Prof. Dr. Shivaram Vaidya

Tri-chandra Multiple Campus

TU, Kathmandu, Nepal

.....

M.Sc. Co-ordinator

Assoc. Prof. Dr. Bhushan Shakya

Department of Chemistry

Amrit Campus, TU

Kathmandu, Nepal

.....

Head of the Department

Prof. Dr. Daman Raj Gautam

Department of Chemistry

Amrit Campus, TU

Kathmandu, Nepal

LETTER OF FORWARD

On the recommendation of **Prof. Dr. Armila Rajbhandari (Nyachhyon)** and **Mr. Naresh Prashad Pant** the dissertation is submitted by **Ms. Sarmila Dangi** Symbol No. 2180/077, T.U. Regd. No.: 5-2-214-34-2016 entitled **"PREPARATION AND CHARACTERIZATION OF COCONUT SHELL DERIVED ACTIVATED CARBON FOR SUPERCAPACITOR APPLICATION"** is forwarded by the Department of Chemistry, Amrit Campus for the approval to the evaluation committee, Institute of Science and Technology (IOST), Tribhuvan University (T.U.), Nepal.

She has fulfilled all the requirements laid down by the Institute of Science and Technology (IOST), Tribhuvan University (T.U.), Nepal for the dissertation.

.....

Tribhuvan University
Amrit Campus
Department of Chemistry

Prof. Dr. Daman Raj Gautam
Head of Department
Department of Chemistry
Amrit Campus

RECOMMENDATION

This is to recommend that **Ms. Sarmila Dangi,** (Symbol. No. 2180., T.U. Regd. No. 5-2-214-34-2016), has carried out a dissertation entitled **"PREPARATION AND CHARACTERIZATION OF COCONUT SHELL DERIVED ACTIVATED CARBON FOR SUPERCAPACITOR APPLICATION"** for the requirement to the dissertation in Master of Science (M.Sc.) degree in Chemistry under our supervision in the Department of Chemistry, Amrit Campus, Institute of Science and Technology (IOST), Tribhuvan University (T.U.), Nepal.

To our knowledge, this work has not been submitted to any other degree.

She has fulfilled all the requirements laid down by the Institute of Science and Technology (IOST), Tribhuvan University (T.U.), Nepal for the submission of the thesis for the partial fulfillment of the Master of Science (M.Sc.) degree in Chemistry.

Tribhuvan University
Amrit Campus
Department of Chemistry

.....

Supervisor

Prof. Dr. Armila Rajbhandari

Central Department of Chemistry

Tribhuvan University

Kathmandu, Nepal

.....

Co-supervisor

Mr. Naresh Prashad Pant

Department of Chemistry

Amrit Campus, TU

Kathmandu, Nepal

DECLARATION

This dissertation entitled **"PREPARATION AND CHARACTERIZATION OF COCONUT SHELL DERIVED ACTIVATED CARBON FOR SUPERCAPACITOR APPLICATION"** is being submitted to the Department of Chemistry, Amrit Campus, Institute of Science and Technology (IOST), Tribhuvan University (T.U.), Nepal for the partial fulfillment of the requirement to the dissertation in Master of Science (M.Sc.) degree in Chemistry. This dissertation is carried out by me under the supervision of Prof. Dr. Armila Rajbhandari (Nyachhyon), Central Department of chemistry, Tribhuvan University, Nepal and co-supervision of Mr. Naresh Prashad Pant in the Department of Chemistry, Amrit Campus, Tribhuvan University (T.U.), Nepal.

This work is original and has not been submitted earlier in part or full in this or any other form to any university or institute, here or elsewhere, for the award of any degree.

.....

Sarmila Dangi
Symbol No: 2180/077
T. U. Regd. No.: 5-2-214-34-2016

ACKNOWLEDGEMENTS

I feel immense pleasure in acknowledging my ineptness and heartfelt sense of gratitude to my respected supervisor Prof. Dr. Armila Rajbhandari (Nyachhyon), Central Department of chemistry, Tribhuvan University, Nepal and co- supervisor Mr. Naresh Prashad Pant, Department of Chemistry, Amrit Campus, Tribhuvan University (T.U.), Nepal for their sustained encouragement, regular guidance, inspiration, valuable suggestion, and great support throughout this period.

My sincere gratitude goes to Prof. Dr. Daman Raj Gautam, Head of the Department of Chemistry, Amrit Campus, Tribhuvan University, Assoc. Prof. Dr. Bhushan Shakya, coordinator of the M.Sc. program in the chemistry department at the Amrit Campus, for providing me with administrative support and necessary laboratory facilities for this dissertation work.

I am deeply grateful to Assoc. Prof. Dr. Ram Lal Shrestha and Assist. Prof. Dr. Deval Prasad Bhattarai for their exceptional assistance in sample preparation and electrochemical characterization, and I extend sincere thanks to Kathmandu Valley School/College for granting access to laboratory facilities.

I am appreciative of Prof. Dr. Leela Pradhan, Department of Physics, Amrit Campus for her kindness in granting us access to the lab spaces, which was essential to the completion of this dissertation.

I would like to express my profound gratitude to Assoc. Prof. Dr. Mahesh Joshi, Central Department of Chemistry, T.U. for his great help in capturing SEM images from China.

I am indebted to all the respected teaching and non-teaching staff of the Department of Chemistry, Amrit Campus, for their direct and indirect help, valuable suggestions, and constant support.

I would like to take this opportunity to thank my classmates Sushila Subedi, Niranjan Ghimire, Puja Thanait, Sirjana Bhattarai, and Sujan Dhital for their kind help and support during my research.

Finally, my deep thanks go to my family and friends for their undying support and faith in me.

Sarmila Dangi

ABSTRACT

Activated Carbon (AC) has been successfully prepared through the chemical treatment of coconut shell (CS) powder followed by a carbonization process at 400 °C for 3 hours in a tube furnace. Phosphoric acid served as the activating agent in a 1:1 ratio by weight of precursor and phosphoric acid. The characterization of as prepared AC was done by Scanning Electron Microscopy (SEM) and Fourier Transform Infrared Spectroscopy (FTIR), along with Methylene Blue (MB_N) and Iodine number (I_N) tests to evaluate porosity. Electrochemical parameters including Cyclic Voltammetry (CV), Galvanostatic Charge-Discharge (GCD) and Electrochemical Impedance Spectroscopy (EIS) were also examined. The SEM analysis revealed a porous morphology. FTIR spectra confirmed the presence of oxygenated surface functional groups such as hydroxyl, carbonyl, and carboxyl. MB_N and I_N methods showed 181.52 mg/g and 821.7 mg/g of MB_N and I_N respectively indicating the presence of mesopores and micropores. The surface area was determined by methylene blue adsorption method and, was found to be 802.12 m^2/g. Electrochemical tests demonstrated promising results. The CV curve was found to be rectangular in shape which indicates Electric Double-Layer Capacitor (EDLC) behavior. The specific capacitance (C_{sp}) was measured by GCD curve which was found to be 136.42 F/g. The energy density (E_d) was also calculated which was found to be significantly high (68.21 Wh/kg) and power density (P_d) was found to be 600 W/kg. EIS results showed a very low resistance of 2.1 Ω. These findings suggest that the laboratory-prepared coconut shell derived activated carbon can be a potential candidate as an electrode material in super capacitive devices.

Keywords: Activated carbon, Coconut shell, Phosphoric acid, Activation, Porosity, Electrochemical properties, Supercapacitor.

शोधसार

यस अध्ययनमा नरिवलको बोक्राको धुलोलाई रासायनिकरुपमा सक्रिय र परिमार्जन गरिएको थियो र ऊर्जा सङ्कलनका लागि तिनीहरुको क्षमता अध्ययन गरिएको थियो । प्रयोगशालामा बनाइएको सक्रिय कार्वनको गुण जाँच्नका निम्ति स्क्यानिङ्ग इलेक्ट्रोन माइक्रोस्कोपी (SEM), फोरियर ट्रान्सफर्म इन्फ्रारेड स्पेक्ट्रोस्कोपी (FTIR), मिथिलिन ब्लु र आयोडिन नम्बर र इलेक्ट्रोकेमिलक अध्ययनहरु; जस्तैः साइक्लिक भोल्टामेट्री (CV), ग्याल्भ्यानोस्ट्याटिक चार्ज डिस्चार्ज (GCD) र इलेक्ट्रोकेमिकल इम्पेडेन्स स्पेक्ट्रोस्कोपी (EIS) प्रयोग गरिएको थियो । वजनको 1:1 अनुपातमा फस्फोरिक एसिडलाई सक्रिय एजेन्टको रुपमा प्रयोग गरी नरिवलको बोक्राको धुलोलाई 400 ^{0}C मा ट्युब फर्नेसमा कार्बोनाइजेशनद्वारा सक्रिय कार्वन तयार गरियो । SEM विश्लेषणले केही दरारहरु अवस्थित भएको छिद्रपूर्ण संचरना देखाएको छ । FTIR स्पेक्ट्राले कार्वोक्सिल, हाइड्रोक्सिल र कार्वोनिलजस्ता अक्सिजनयुक्त सतह कार्यात्मक समूहहरुको उपस्थिति पुष्टि गऱ्यो । पोरोसिटी मापनले क्रमशः 181.52 mg/g , 821, 7 mg/g को मेजोपोरोसिटी र माइक्रोपोरोसिटी संकेत गऱ्यो । सतह क्षेत्र पनि मिथाइलिन ब्लु नम्बरबाट निर्धारण गरिएको थियो, जुन 802.12 m^2/g पाइयो । इलेक्ट्रोकेमिकल परीक्षणहरुमा CV लगभग आयातकार थियो, जसले इलेक्ट्रिक डबल लेयर क्यापासिटर (EDLC) व्यवहार जनाउँछ । GCD ले 68.21 Wh/kg को ऊर्जा घनत्व र 600 W/kg को पावर घनत्व साथै 136.42 F/g को एक विशिष्ट क्यापेसिटन्स देखायो । EIS परिणामले 2.1 Ω को प्रतिरोध प्रदर्शन गऱ्यो । यी निश्कर्षहरुले सुझाव दिन्छन् कि प्रयोगशालामा तयार नरिवलको बोक्राबाट व्युत्पन्न सक्रिय कार्वनको सुपर क्यापासिटिव उपकरणहरुमा इलेक्ट्रोड सामाग्रीको रुपमा सम्भावित अनुप्रयोगहरु छन् ।

शब्द कुञ्जिका : सक्रिय कार्वन, नरिवलको बोक्रा, फस्फोरिक एसिड, सक्रियता, पोरोसिटी, इलेक्ट्रोकेमिकल गुणहरु, सुपरक्यापासिटर

LIST OF ACRONYMS AND ABBREVIATIONS

AC : Activated carbon

MB : Methylene blue

ppm : Parts per million

rpm : Rotation per minute

I_N : Iodine adsorption number

MB_N : Methylene blue number

FTIR : Fourier Transform Infrared Spectroscopic analysis

SEM : Scanning Electron Microscopy

CV : Cyclic Voltammetry

GCD : Galvanostatic Charge- Discharge

EIS : Electrochemical Impedance Spectroscopy

CS-1 : Raw sample

CS-2 : Acid treated sample

CS-3 : As prepared activated carbon

CS : Commercial sample

G **:** Gram

nm : Nanometer

µm : Micrometer

hrs **:** Hours

s **:** Second

A/g **:** Ampere per gram

F/g : Faraday per gram

W/kg **:** Watt per kilogram

Wh/kg **:** Watt hour per kilogram

m^2/g **:** Meter square per gram

mg/g **:** Milligram per gram

mg/L **:** Milligram per litre

mV **:** Millivolt

C_{sp} **:** Specific capacitance

E_d **:** Energy density

P_d **:** Power density

Z' : Real resistance

Z'' : Imaginary resistance

°C **:** Degree centigrade

μ : Micro

λ : Lamda

Δ : Delta

ε : Epsilon

Ω : Ohm

& : And

LIST OF TABLES

LIST OF FIGURES

TABLE OF CONTENTS

CHAPTER-1

INTRODUCTION

1.1 General Introduction

Carbon-based materials particularly in their activated form, are commonly employed in various aspects of environmental analyses, like purification and pollution remediation, renewable energy generation and storage mechanisms (Titirici et al., 2015). The examples of energy storage are supercapacitors, solar cells, batteries and sensors as well. These materials, including powders, fibers, composites, monoliths, and foils, are distinguished by their high specific surface area, considerable pore volume, mechanical stability, and chemical inertness (Frackowiak, 2007). The term “activated carbon (AC)” commonly denotes carbon compounds that differ from pure carbon because of oxidized carbon atoms present on their exterior and interior surfaces. These materials are characterized by their high porosity, stability in various conditions, ability to adsorb substances effectively, strong mechanical properties, notable surface reactivity, and extensive surface area (Yahya et al., 2015). Commercial AC can be made from non-renewable materials such as coal, wood, and synthetic polymers. These substances typically possess characteristics such as low mineral content, high porosity, and significant carbon content. Scientists are currently exploring affordable biowaste alternatives and methods for producing AC, considering their impact on both the environment and the economy (Muttil et al., 2023). Low-cost resources with high carbon content and low inorganics have been utilized as raw materials in the synthesis of activated carbon. Scientists have been researching eco-friendly, low-cost carbon compounds, with a particular emphasis on the potential utilization of plant and animal waste. A potential approach is utilizing waste lignocellulosic materials for low-cost AC production.

A carbonaceous material mainly comprises carbon elements. Carbon's electronic arrangement ($1s^2$, $2s^2$, and $2p^2$) allows for unique bonding with other elements and itself. It exists in different allotropic forms among them **Fig. 1** shows three common allotropic forms produced when it bonds with other carbon atoms (Yahya et al., 2018).

I. Hexagonal graphite - A layered structure of graphene formed when carbon atoms bond via σ-bonds and π-bonds with three neighboring carbon atoms, resulting in a sp^2 based configuration.

II. Fullerene (C_{60}) - A three-dimensional structure formed when the bonds between carbon atoms bend, creating an empty cage composed of sixty (C_{60}) or more atoms, leading to $sp^{2+\varepsilon}$ based configuration.

III. Cubic diamond - A solid and uniform three-dimensional framework created when every carbon atom forms four σ-bonds with four neighboring carbon atoms, leading to a sp^3 based configuration.

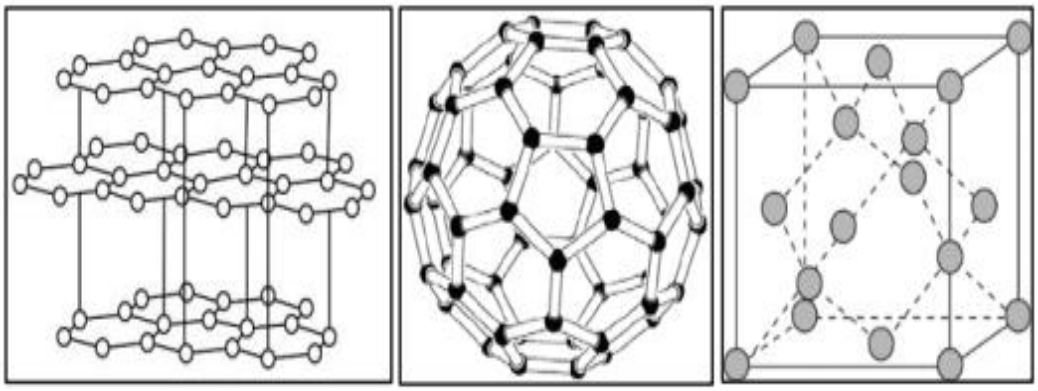

Figure 1: Allotropic forms of hexagonal graphite (left), fullerene (middle) and cubic diamond (right) (Yahya et al., 2018).

Carbon allotropes with a graphite-like structure are more abundant on the atomic scale than those with diamond-like or fullerene structures (Ren et al., 2013). AC is classified as non-graphitized graphite carbon due to its porous nature and low density. AC's chemical properties are determined by the presence of heteroatoms on its surface, such as hydrogen, oxygen, nitrogen, phosphorus, and sulfur. These heteroatoms and delocalized electrons form new functional groups during activation, determining whether AC is acidic or base (Aygün et al., 2003; Shafeeyan et al., 2010).

Syeda and colleagues (Ali et al., 2019) documented a variety of surface functional groups, including carbonyl, carboxylic, and ether groups. The International Union of Pure and Applied Chemistry (IUPAC) classifies AC pores into three types: micropores (< 2 nm), mesopores (2 nm – 50 nm), and macropores (> 50 nm) as shown in **Fig. 2** (Hasdi1 et al., 2023).

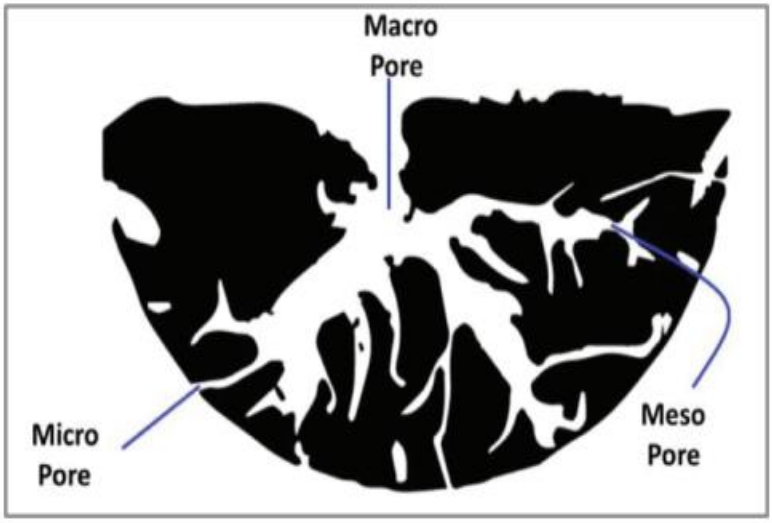

Figure 2*:* Different types of pores in AC (Hasdi1 et al., 2023).

1.2 Precursor for AC

This study aims to produce nanoporous activated carbon from eco-friendly materials. In this context, lignocellulosic materials were investigated for the synthesis of AC. Lignocellulosic biomass is primarily composed of three components: cellulose, hemicellulose, and lignin which is shown in **Fig.3**. Lignin, the predominant constituent, plays a crucial role in adsorption mechanisms. Many precursors such as rice husk (Shrestha et al., 2021), almond shell (Plaza et al., 2010), walnut shell, waste tea, tamarind seeds (Banu et al., 2016), waste sawdust (Shrestha et al., 2018), coffee ground waste (Adan-Mas et al., 2021), coconut shells (Sujiono et al., 2022) have been extensively used to prepare AC.

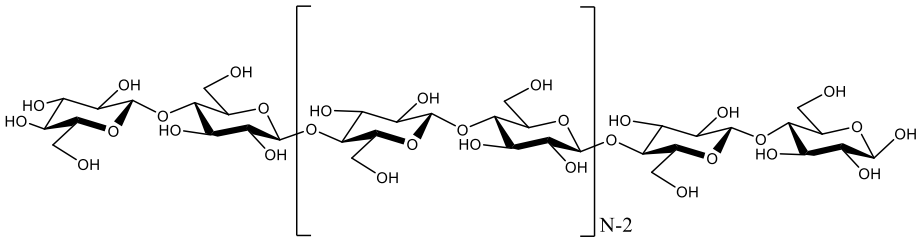

Cellulose

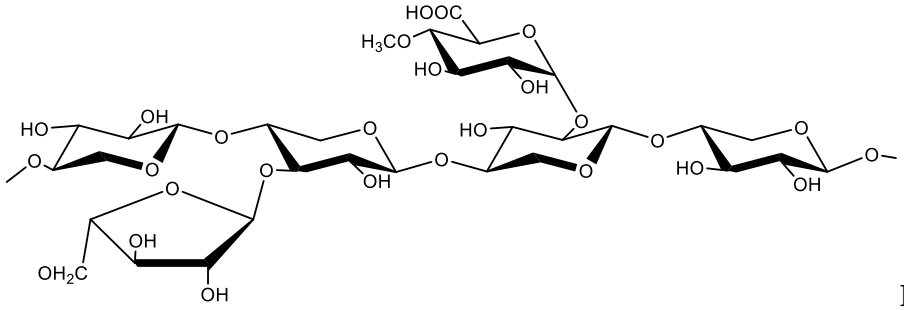

Hemicellulose

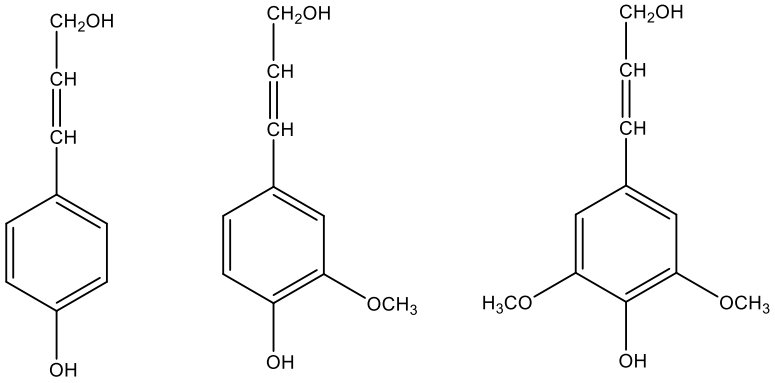

Lignin

Figure 3: Structures of cellulose, hemicellulose and lignin found in lignocellulosic material

In this study, Coconut shells have been studied as the precursor for the production of AC. Coconut (*Cocos nucifera*) is a part of the Arecaceae (Palmae) plant family (Obidoa et al., 2010). They are grown mostly in tropical places with high humidity, consistent rainfall, and sandy soil. A recent study discovered that the coconut product industry is quickly growing because of its antiviral properties, which are highly effective in treating COVID-19. Minerals like sodium, iron, calcium, magnesium, phosphorus, and selenium are found alongside vitamins C, E, B1, B3, B5, and B6 (Henrietta et al., 2022). Coconut yields various by-products such as coconut water, recognized as a health powerhouse for reinforcing the immune system and possessing antifungal, antiviral, anti-parasitic, and antibacterial properties (Akpro et al., 2019). Coconut oil contributes to cardiovascular health, blood sugar management, and cognitive performance in

Alzheimer's patients (Henrietta et al., 2022). Coconut milk finds uses in both the culinary and beauty industries. Additionally, raw coconut is consumed as a fruit. A huge amount of coconut is produced in Nepal; thus, large amounts of coconut shells are produced as waste byproducts across various industries annually. Due to its origin from agricultural production, its waste is generally regarded as agricultural waste. Coconut shell's high cellulose (approximately 23-43%) and lignin content (35-45%) make it a promising precursor for AC production (Agbozu et al., 2014). Therefore, in the present study, coconut shell waste, an abundant and inexpensive waste bio-material was chemically modified by treating it with phosphoric acid and was carbonized for the production of AC. **Fig. 4 (a)** depicts a coconut tree. Similarly, **Fig. 4 (b)** shows the coconut fruit, while **Fig. 4 (c)** represents the coconut shells.

Figure 4: Various forms of coconut **a)** Coconut tree, **b)** Coconut fruit, and **c)** Coconut shells.

1.3 Synthesis and Activation of Activated Carbon (AC)

As previously stated, AC can be produced using high-carbon content materials such as seeds, wood and agricultural wastes. Before activation, these materials are washed, dried, milled, sieved, and demineralized using acidic or basic solutions. AC must have the least amount of ash and minerals to function as a catalyst. This process ensures efficient AC production. The next stage involves subjecting the materials to carbonization, a process aimed at eliminating non-carbon elements (volatile components) and converting the organic matter into elemental carbon. During this phase, any substance containing significant carbon content undergoes pyrolysis within a temperature range of 600 °C to 1000 °C, typically carried out in an inert atmosphere using gases such as nitrogen (N_2) or argon. Enhancing the porous nature of AC obtained from carbonization involves several activation stages aimed at increasing pore volume, diameter, and surface area. This process involves removing disordered carbon and treating lignin with the activating agent. As a result, pores expand as the walls between

them are burnt away, leading to greater provisional pores and microporosity. The activation phase is widely recognized as the key preparation step for porous carbon (Naji & Tye, 2022; Nor et al., 2013). Activation could be physical or chemical.

1.3.1. Physical Activation

In the physical activation of carbonaceous materials, a two-step approach is commonly employed. Once the carbonization phase is completed, the resulting char undergoes activation by exposure to oxidizing gases such as CO_2 and steam or air mixture at elevated temperatures ranging from 800 °C to 1000 °C. This procedure aims to create a high surface area with a complex porous structure through the following reactions (Mazlan et al., 2016):

$$C + O_2 \longrightarrow CO_2$$

$$C + CO_2 \longrightarrow 2CO$$

$$C + H_2O \longrightarrow CO_2 + 2H_2$$

Physical activation has several advantages over chemical activation, including cheaper activation costs and no chemical waste (Pallarés et al., 2018). In contrast, the main disadvantages of physical activation are the extended activation time and high energy consumption caused by the dual cooling phases. Furthermore, given that the high temperature required (up to 1000 °C) during activation, the AC generated by this approach lacks certain properties, rendering it unsuitable as a catalyst, adsorbent, or filter (Yahya et al., 2015)

1.3.2. Chemical Activation

Chemical activation is a one-step technique that generates activated carbon from cellulose-rich materials such as wood and fruit pits (Yahya et al., 2015). Carbonaceous materials are impregnated with chemical agents before being activated and carbonized at moderate temperatures (400 °C–900 °C). This approach has advantages such as minimal energy consumption, a rapid activation period, and a large surface area of up to 3000 m^2/g (Abd et al., 2020). However, the primary drawback of the chemical activation method lies in the contamination of wastewater resulting from the chemical washing. The process is influenced by a variety of characteristics, including the activating agent and temperature used, the impregnation method, and the gas flow

during carbonization (Yorgun et al., 2016). Because of the advantages that it offers, chemical activation is preferred over physical activation.

1.4 Applications of Activated Carbon (AC)

Activated carbon finds diverse applications in addressing environmental pollution, industrial needs, and energy utilization. Renowned for its exceptional adsorption capabilities, activated carbon effectively eliminates various contaminants like dyes, heavy metals, and pesticides from both air and water sources (Wong et al., 2018). Its usage extends to purifying, detoxifying, deodorizing, and decolorizing water bodies. Recent scientific attention has also focused on utilizing activated carbon across industries including food, pharmaceuticals, chemicals, oil, and mining, particularly in water treatment processes. Moreover, it plays a vital role in energy-related domains such as battery technology, solar cells, sensors, and supercapacitors (Marpaung et al., 2019). This study primarily explores the utilization of activated carbon in supercapacitors.

1.4.1. Supercapacitors

The rising energy demand has led to a critical need for the global science and technology communities to prioritize the development of clean, sustainable, and highly efficient technologies for storing and converting energy. Batteries, fuel cells, and supercapacitors (SCs) are examples of electrochemical energy storage and conversion technologies that have been acknowledged as significant. Scientists have been interested in supercapacitors, a family of efficient energy storage devices with high power and high energy density, a long lifespan cycle, outstanding charge and discharge rates, low input resistance, extended lifetime, and environmentally friendly (Şahin et al., 2022). Over the past decade, numerous hybridization configurations have been suggested and utilized to enhance the power density and lifespan of energy storage systems (Chen et al., 2009). Recent advancements have prompted a comparison between supercapacitors (SCs) and rechargeable batteries, as they compete for dominance in energy storage technologies (Abdel Maksoud et al., 2021). Consequently, there has been a surge in research exploring the electrochemical properties of various materials and their composites, with potential applications in future lithium-ion batteries. SCs offer a promising alternative for storing electrical energy in solid-state devices, aiming to address several limitations associated with conventional batteries (Lee et al., 2021).

Supercapacitors can be broadly classified into three categories: hybrid capacitors, pseudo-capacitors, and electrochemical double-layer capacitors (EDLCs). EDLCs employ a non-Faradaic electrostatic charge storage mechanism, relying on physical charge separation at the electrode-electrolyte interface (Gopalakrishnan & Badhulika., 2020), while pseudo-capacitors store energy through reversible faradaic redox reactions on the electrode (Şahin et al., 2022). Hybrid capacitors, blending features of both pseudo-capacitors and EDLCs, offer increased energy and power density through synergistic interactions. In terms of precursor availability and performance, EDLC-type supercapacitors are emerging as prominent choices for power backup applications. They feature high power density, extended lifespan, and cost-effectiveness in precursor materials, making them increasingly preferred for various energy storage needs. **Fig. 5** shows the electrochemical double layer (EDLC).

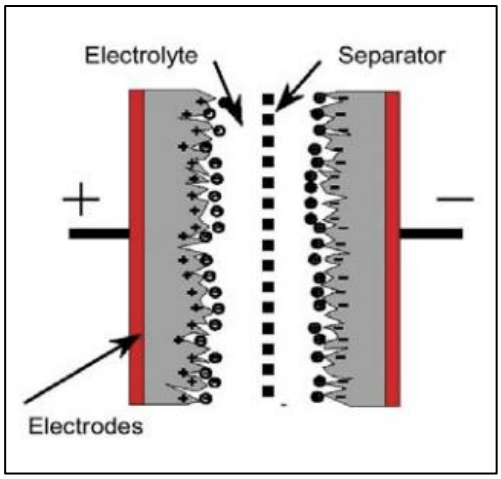

Figure 5: Schematic diagram of EDLC type supercapacitor (Wasterlain et al., 2006).

The basic composition of a supercapacitor includes aluminum current collectors and electrodes typically made of activated carbon infused in either an organic or aqueous electrolyte. A separator is placed between the electrodes to provide insulation as shown in **Fig. 5** (Wasterlain et al., 2006). Supercapacitors disperse ions from the electrolyte close to the electrode-electrolyte contact to store energy. Electrostatic energy storage is made possible by the creation of a double electric layer when applied to a terminal voltage. Supercapacitors have a higher surface activation than conventional capacitors because of their anode-cathode construction with activated carbon. High capacities (1 to 5000 F) are possible with this, making it perfect for use as a supplement to batteries or fuel cells for storage. Because supercapacitors employ parallel-series designs, many cells can output voltage and current, which makes them perfect for fuel cells or batteries

(Zhang & Zhao, 2009). The capacitance developed (C) between the electrode and electrolyte intersection is given by the Helmholtz double layer concept (Zhang & Zhao, 2009).

$$C=\frac{\varepsilon_r \varepsilon_o}{d} A \qquad \text{…….... (1)}$$

Where, ε_r is the electrolyte dielectric constant, ε_o is the permittivity of a vacuum, A is the specific surface area of the electrode accessible to the electrolyte ions, and d is the effective thickness of the EDLC. Specific surface area and specific capacitance should be correlated linearly, according to **equation (1)**.

Because of their impressive power density and versatility, supercapacitors (SCs) find applications across various fields such as industrial processes, mobile base stations, wind turbines, and electronic devices (Bottu et al., 2013; Kuperman et al., 2013). Their superiority over lead-acid batteries also makes them viable options in power electronics, electric vehicles, and UPS systems. Moreover, besides powering flashes and decreasing energy usage and CO_2 emissions in transportation networks, SCs can also stabilize power supply amidst fluctuating loads (Şahin et al., 2022).

In recent years, a variety of carbon materials have become popular choices for electrode materials in supercapacitors, including activated carbon (AC), carbon nanotubes, carbon nanofibers, graphene sheets, and others. Specifically, activated carbon with its porous structure and high specific surface area has gained significant interest due to its outstanding attributes such as low cost, simple preparation, excellent chemical stability, and high electrical conductivity.

In this study, we are analyzing the electrochemical properties of AC prepared from waste coconut shells as its potential use as an electrode material in supercapacitors.

1.5 Characterization of Activated carbon

1.5.1. Scanning Electron Microscopy (SEM)

Scanning Electron Microscopy, commonly referred to as SEM, is a powerful imaging technique used in various fields of science and engineering to observe the surface morphology and structure of materials at incredibly high resolution. SEM employs a focused beam of electrons that reacts with a sample to produce secondary electrons, backscattered electrons, and x-rays, which are then analyzed to provide a topographical

image and relative composition of the sample under investigation (Abdullah & Mohammed, 2019)

1.5.2. Fourier Transform Infrared Spectroscopy (FTIR)

Fourier Transform Infrared spectroscopy (FTIR), is a valuable method for identifying different surface functional groups. It's highly sensitive and non-destructive, relying on the absorption strengths of various functional groups across different wavenumbers in the near-infrared range. By observing spectra resulting from IR wavelength absorption, analysts can determine the functional groups within a sample. Absorption happens when the IR frequency matches the vibrational frequency of a bond, indicating the presence of IR active compounds in the spectra (Ismail et al., 1997).

1.5.3. Iodine Number (I_N)

The method employed to measure the porosity of activated carbon is known as the iodine number. It represents the amount of iodine, measured in milligrams, adsorbed by one gram of carbon. Since iodine particles are small and similar in size to micropores, the iodine number serves as an indicator of the concentration of micropores within the AC. The iodine number is determined by assessing the capacity of reactivated or unused carbons to adsorb iodine from a solution. The fundamental reaction between iodine and unsaturated carbon can be represented as;

$$H_2C{=}CH_2 + I_2 \longrightarrow H_2IC\text{-}CH_2I$$

One mole of iodine corresponds to one mole of carbon-to-carbon double bond. This illustrates that the degree of unsaturation rises alongside the iodine number (Nunes & Guerreiro, 2011). It is calculated by using the formula;

$$I_N = \frac{\text{Amount of iodine adsorbed by carbon}}{\text{Mass of activated carbon}} \quad \ldots\ldots\ldots\ldots \textbf{(2)}$$

1.5.4. Methylene Blue Number (MB_N)

The methylene blue number indicates the quantity of methylene blue, measured in milligrams, adsorbed by one gram of carbon, providing insights into the presence of mesopores. It is stated as grams of methylene blue per gram of adsorbent. The selection of methylene blue is based on its strong tendency to adsorb onto solids. It is calculated using the **equation (3)** (Raposo et al., 2009).

$$MB_N = (C_1 - C_2) \times V/M \qquad \ldots\ldots\ldots\ldots\ldots\ldots \textbf{(3)}$$

Where, C_1= Initial concentration of MB

C_2= Equilibrium concentration of MB

V= Volume of solution

M= Mass of adsorbent

The concentration of the MB solution at equilibrium time (C_2) is calculated using the **equation (4)**.

$$C_2 = \text{Absorbance/ Slope} \quad \ldots\ldots\ldots\ldots\ldots \textbf{(4)}$$

1.5.5. Surface Area Determination

The determination of the surface area of AC is commonly carried out using the methylene blue adsorption method. Methylene blue, also known as basic blue 9, tetramethylthionine chloride, is a synthetic cationic thiazine dye with the chemical formula $C_{16}H_{18}ClN_3S$. In its powdered form, it appears dark green, but in an aqueous solution, it exhibits a distinctive deep blue color as it dissociates into an MB cation $[C_{16}H_{18}N_3S]^+$ and a chloride anion $[Cl]^-$. The cationic form of methylene blue is utilized to adsorb acidic sites on the adsorbent material.

The surface area of AC was determined using the formula;

$$S_{MB} = (Q_m \times a_{MB} \times N)/M \quad \ldots\ldots\ldots\ldots\ldots \textbf{(5)}$$

Where,

S_{MB} = Surface area

Q_m = Maximum loading

a_{MB} = Cross section area of one molecule of MB = 197.2×10^{-20}

N = Avogadro's number = 6.023×10^{23}

M = Molecular weight of MB = 319.84 g/mol

The maximum loading (Q_m) of MB on the adsorbent sample can be obtained by using the Langmuir adsorption isotherm. Then surface area can be calculated by using **equation (5).**

1.5.5.1. Langmuir isotherm model

The Langmuir adsorption isotherm is a widely recognized model for describing adsorption phenomena. It suggests that adsorption occurs in a monolayer on a solid

surface with uniform and identical sites. Once these sites are occupied by the adsorbate, further adsorption ceases, indicating a state of saturated monolayer adsorption (Chang et al., 2020).

The Langmuir adsorption equation can be expressed by the following formula:

$$Q_e = (Q_m b C_e) / (1 + bC_e) \quad \text{……} \textbf{(6)}$$

The linear form of Langmuir expression is written as:

$$C_e/Q_e = (1/Q_m b) + (C_e/Q_m) \quad \text{……} \textbf{(7)}$$

Q_e can be calculated using the **equation (8)**;

$$Q_e = (C_0 - C_e) \times V/M \quad \text{…….....} \textbf{(8)}$$

Where,

Q_e (mg/g) is the amount of adsorbate adsorbed per unit mass of adsorbent

M (g) is the mass of the adsorbent

V (L) is the volume of the solution treated

C_0 (mg/L) is the initial concentration of the solution

C_e (mg/L) is the equilibrium concentration of the adsorbate in solution after adsorption

Q_m (mg/g) is the maximum amount of biosorption that can occur with complete monolayer coverage on the biosorbent surface

b (L/mg) is the Langmuir constant

The values of Q_m and b are calculated from the slope and intercept of the C_e/Qe versus C_e plot.

1.6 Electrochemical Characterization

1.6.1. Cyclic Voltammetry (CV)

Cyclic voltammetry (CV) is an electrochemical technique where a triangular voltage waveform is applied to measure the current response of a stationary electrode in a solution. The potential changes linearly with respect to a reference electrode. When the potential reaches its limits, the direction of the scan is reversed, and the potential returns to its original value. This process is repeated multiple times, with the voltage extrema

where reversal occurs known as switching potentials. In each experiment, the oxidation or reduction of analytes may be diffusion-controlled. The initial scan direction can be either positive or negative depending on the sample composition, and the opposite direction is termed the reverse scan. The cycle periods typically range from 1 millisecond to 100 seconds. Finally, the resulting current at the working electrode is plotted against the applied voltage to generate a cyclic voltammogram. CV curves for EDL-based capacitors typically resemble rectangular shapes with constant current (Bhoyate et al., 2019).

1.6.2. Chronopotentiometry

Chronopotentiometry, formerly known as constant current voltammetry, is a technique that involves measuring and interpreting potential-time curves. In this method, a small current is passed through a cell containing a working electrode and an auxiliary electrode. The potential changes of the working electrode are monitored against a reference electrode. Sufficient supporting electrolyte is added to the cell to ensure that the electroactive species is transported solely by diffusion. The potential changes of the working electrode are then plotted against time, resulting in a chronopotentiogram. This technique finds applications in analytical chemistry and is particularly useful for studying electrode kinetics. One of its applications is in determining specific capacitance. The specific capacitance (C_{sp}) indicates how much electric charge a material can hold per unit area for a given applied voltage. It is calculated by using **equation 9**:

$$C_{sp} = \frac{I\Delta t}{m\Delta V} \qquad \text{…….……. (9)}$$

Energy density refers to the amount of energy stored per unit volume or mass within a given material or system. Similarly, power density measures how much power can be generated, stored, or transmitted within a certain volume or mass. To calculate energy density and power density following equations are used:

$$E_d = \frac{1}{2} \times C_{s_P} \times (\Delta V)^2 \quad \text{…….…. (10)}$$

$$P_d = \frac{E}{\Delta t} \qquad \text{…….. (11)}$$

Where,

C_{sp} = Specific capacitance

I = Constant Current

Δt = Discharge time

m = Mass of activated carbon

ΔV = Potential window

E_d = Energy density

P_d = Power density

1.6.3. Electrochemical Impedance Spectroscopy (EIS)

Electrochemical Impedance Spectroscopy (EIS) is a powerful technique used to assess the electrical properties of electrochemical systems. It entails applying a low-amplitude sinusoidal signal of voltage or current across the system across a spectrum of frequencies and analyzing the impedance response. EIS finds broad application in the examination of corrosion, batteries, fuel cells, sensors, and various electrochemical processes. It offers valuable insights into the electrical characteristics of electrochemical interfaces, including solution resistance, charge transfer resistance, and double-layer capacitance.

The Nyquist plot, an essential tool in Electrochemical Impedance Spectroscopy (EIS), visually depicts the impedance characteristics of electrochemical systems. It plots the real part of impedance (Z') against the negative of the imaginary part (-Z") on a complex plane. In the case of Electric Double Layer Capacitors (EDLCs), the Nyquist plot exhibits specific patterns that exhibit the electrochemical behavior of the system: a linear section at low frequencies signifies diffusion-limited processes (Warburg impedance), a semicircular shape at higher frequencies corresponds to charge transfer resistance (Rct) and solution resistance (Rs), a capacitive loop at intermediate frequencies indicates double-layer capacitance, and at very high frequencies, there's a tendency towards purely capacitive behavior (Shrestha et al., 2019). Analysis of the Nyquist plot offers valuable insights into EDLC characteristics, aiding in their optimization for diverse applications such as energy storage in electronics and electric vehicles.

CHAPTER-2

LITERATURE REVIEW AND RESEARCH GAP

2.1 Literature Review

Activated carbon (AC) was produced commercially in Europe in the 19th century and was widely used in the sugar business. In 1936, it was used in water treatment processes in the United States. Since, then it has got wide applications in various fields including pollution control, the treatment of groundwater, the adsorption of contaminants from the air and water, and the elimination of heavy and trace metal ions from solutions. The majority of AC, that is sold commercially comes from coal or petroleum, which makes it expensive. Hence, researchers are constantly looking for cheap ways to produce AC. Fruit shells and stones are some examples of lignocellulosic materials derived from agriculture that may be used sustainably to produce AC (Ioannidou & Zabaniotou, 2007).

A study focused on converting lignin into valuable activated carbon due to its abundance, low cost, and unique properties. Various preparation methods were explored to optimize pore structure and enhance adsorption capacity, including chemical, physical, and physicochemical techniques. These methods aimed to address challenges related to pore structure, specific surface area, and pore size distribution. Lignin-based activated carbon found extensive applications in gas purification, wastewater treatment, electrodes, and supercapacitors, highlighting its potential for value-added utilization (Dong et al., 2023).

Also, the study on the preparation of activated carbon from peach stone impregnated with pyrophosphoric acid ($H_4P_2O_7$) was reported using a one-step carbonization procedure and varying conditions to optimize preparation parameters. The study systematically explored the impact of activation duration, initial concentration of activating agents, activation temperature, and soaking duration on the production of peach stone derived activated carbon (PSAC). The model adsorbate, AR18 dye, was used to assess the adsorption capability of the produced PSAC. It showed a higher iodine value (1274 mg/g). Analytical studies demonstrated that the PSAC was produced with a high surface area and a mostly microporous nature for improved adsorption (Saratale et al., 2016).

Similarly, another study utilized corncob as the raw material and employed bio-oil as the activating agent for the preparation of activated carbon. The research focused on examining the influence of activation temperature and the specific type of activating agent on the adsorption properties. Activated carbon produced via bio-oil activation shows a high yield but poor adsorption performance due to underdeveloped pore structure and surface alkali/alkaline earth metal content. Wood vinegar-activated carbon outperforms phosphoric acid-activated carbon at 450 °C and 650 °C. At 850 °C, wood vinegar-activated carbon achieves a specific surface area of 384.35 m^2/g and methylene blue adsorption capacity of ~45 mg/g, surpassing phosphoric acid-activated carbon. This suggests wood vinegar as a superior activator. Using organic acid solutions like biomass pyrolysis liquid offers an eco-friendly approach to activated carbon preparation and a new route for pyrolysis liquid utilization (Feng et al., 2020).

Activated carbon with a notably large surface area was produced from coconut shells through chemical activation, using KOH as the activating agent. Surface area and pore volume were determined using the BET method, Langmuir equation, and t-plot method. Results revealed impressive values of 2451 m^2/g for surface area and 1.21 cm^3/g for pore volume. These activated carbons demonstrated significantly enhanced adsorption capabilities for phenol, 4-chlorophenol, and 4-nitrophenol from aqueous solutions compared to commercially available activated carbon (Hu & Srinivasan, 1999).

This study investigated producing activated carbon from durian rind waste, with an emphasis on increasing surface area and oxygen groups. Numerous activation techniques were investigated; hydrothermal and acid activation demonstrated positive results, especially in terms of increasing iodine number. The best preparation conditions were found by using the Box-Behnken design, with temperature, the solid/water ratio, and the solid/acid ratio being the three most important factors. The maximum iodine number of 626.47 mg/g was obtained by response surface methodology (RSM) and closely confirmed experimentally at 666.73±6 mg/g. Increased oxygen content was found on the activated carbon surface in the form of carbonyl and sulfonyl groups, according to functional group analysis using FTIR (Sriprom et al., 2021).

The research aimed to develop cost-effective composite materials by combining activated carbon with metallic nanoparticles (MNPs) of copper (Cu), silver (Ag), and iron (Fe). MNPs were applied onto activated carbon using ultrasound and subsequent

treatment with $NaBH_4$ as a reducing agent. Various analytical techniques, including XRD, XRF, FTIR, XPS, TGA, SEM, and TEM, were utilized to analyze and confirm the properties of the materials. These composites were then assessed as catalysts for reducing organic pollutants like MB, MO, and 4-NP in both single and combined systems using $NaBH_4$. The metal nanoparticle concentrations were found to be 2.12%, 11.15%, and 12.13% for AC-Ag, AC-Cu, and AC-Fe, respectively. TEM analysis showed differences in nanoparticle sizes and distribution, particularly with AC-Cu displaying ultrafine particles ranging from 4 to 14 nm. Optimization efforts focused on catalyst type, $NaBH_4$ concentration, pollutant concentration, catalyst mass, and pollutant type. AC-Cu emerged as the most effective catalyst, attributed to the dispersion of CuNPs. Moreover, the AC-Cu catalyst maintained its efficiency in MB reduction over five consecutive cycles (Boukoussa et al., 2024).

Similarly, a study compared one-step and two-step approaches to investigate the effects of carbonization on the synthesis of activated carbon utilizing materials based on petroleum coke. It studied how surface morphology, pore structure, and iodine adsorption efficiency were affected by the carbonization temperature range of 550–750 °C and the activation heating rate of 10 °C/min and 20 °C/min. Findings showed that pre-carbonization reduced the amount of functional groups on the surface that contained oxygen. Higher heating rates (20 °C/min) resulted in more functional groups containing oxygen and a delay in pore merging. Specific surface area was reduced by up to 55.5% after carbonization, not increased. Carbonized activated carbon, on the other hand, demonstrated enhanced microporous structure at a heating rate of 20 °C/min. As demonstrated by iodine adsorption values, micropore width rather than specific surface area impacted iodine adsorption performance (Feng et al., 2024).

In the same way, using zinc chloride and vacuum chemical activation, walnut shells have been converted into activated carbons. Investigations were conducted into the effects of pore volume and specific surface area on activation temperature, system pressure, and impregnation ratio. A 2.0 impregnation ratio, 30 kPa pressure, and 450 °C temperature were the ideal parameters for producing activated carbon, which had a total pore volume of 1.176 cm^3/g and a BET surface area of 1800 m^2/g. After performing SEM, TEM, and FTIR characterization, the performance of the activated carbon in removing methylene blue was evaluated. A favorable connection was observed between the maximum adsorption capacity of 315 mg/g and BET surface area.

The Redlich-Peterson and Langmuir-Freundlich models gave the best depiction of the adsorption isotherms that were studied, suggesting heterogeneous surface adsorption (Yang & Qiu, 2010).

In recent years, carbon materials derived from biomass have gained attention for their exceptional electrochemical properties, cost-effectiveness, and sustainability. They have been utilized in various applications such as supercapacitors and solar cells, offering advantages like adjustable porosity and morphology for enhanced performance. This review explored the progress in utilizing biomass-derived carbon electrodes for energy storage and conversion devices, highlighting their potential in integrated power packs. The discussion included the storage properties of supercapacitors and the photovoltaic parameters of solar cells based on biomass-sourced carbons, as well as the efficiency of solar cell-supercapacitor integrated devices (Keppetipola et al., 2021).

Moreover, once discarded after the extraction of herbs, kochia has shown value because of its tubular structure and lignocellulosic richness. It produced a graded porous carbon-based supercapacitor electrode material with a rich microstructure and a specific surface area of 1441.30 m^2/g after going through high-temperature pyrolysis and activation. It maintained 90.31% capacitance after 10,000 cycles in a 6 M KOH electrolyte, demonstrating a specific capacitance of 284 F/g at 1 A/g current density. It demonstrated strong cycling stability in symmetrical supercapacitors, maintaining 88.83% after 10,000 cycles and achieving an energy density of 12.3 Wh/kg at 300 W/ kg power density. This shows that waste biomass can be sustainably transformed into stable, high-capacitance supercapacitors (Fan et al., 2023).

Brown seaweeds called *Turbinaria turbinata* were investigated as a possible carbon electrode material for symmetric electrochemical supercapacitors. The electrochemical properties of the carbon materials were assessed using electrochemical impedance spectroscopy, galvanostatic charge/discharge technique, and cyclic voltammetry. According to preliminary results, the sample obtained by pyrolysis at 800 °C performed at its best, with an average surface area of 812 m^2/g. A particular series resistance of 0.5 Ω cm^2, an ionic resistivity of 1.3 Ω cm^2, and a capacitance of 74.5 F/g was measured by electrochemical evaluations with an organic electrolyte. These findings highlighted

the carbon produced from seaweeds remarkable capacitive properties and their prospective application in electrochemical supercapacitors (Pintor et al., 2013).

In a recent study, the leftover leaf material of *Coffea canephora* was chemically activated by conventional pyrolysis at high temperatures to produce activated carbon for supercapacitor electrodes. The activating agent was different concentrations of KOH. When compared to other concentrations, the activated carbon produced with 0.3 M KOH showed better electrochemical performance and physicochemical characteristics. In 1 M H_2SO_4 and 1 M Na_2SO_4 electrolytes, it demonstrated specific capacitances of 297 F/g and 220 F/g at 1 A/g, respectively. This study provides information on how to improve activated carbon's performance as supercapacitor electrode materials for energy storage systems that use renewable resources (Taer et al., 2023).

The goal of the study was to repurpose waste biomass by employing an H_3PO_4 based activation process to produce sawdust-derived activated carbon (SD-AC). Due to its hierarchically porous structure, which has a pore volume of 0.35 cm^3/g and a large specific surface area of 621 m^2/g, SD-AC performed better electrochemically. The SD-AC electrode showed exceptional rate capability (129.06 F/g at 20 A/g), cycling stability (maintaining 87% capacity over 10,000 cycles at 10 A/g), and highest specific capacitance of 244.1 F/g at 1.0 A/g. Furthermore, a peak energy density of 19.9 Wh/kg at a power density of 650 W/kg was attained by the symmetric supercapacitor that used SD-AC, highlighting the potential of waste biomass for efficient energy storage applications (Zhou et al., 2022).

The study investigated the suitability of steam-activated carbon from coconut shells and its acid-washed variants for high-power supercapacitors. Acid washing, particularly with HF, improved the carbon's structure and purity. The HF used AC variant exhibited optimal properties, facilitating fast electrolyte ion diffusion. Two-electrode measurements showed an electrode capacitance of 162 F/g and an energy density of 35.2 Wh/kg at 1 A/g, with a power density of 3967 W/kg at 10 A/g, and excellent cycling stability, retaining 96% of initial capacitance after 5000 cycles at 10 A/g (Ashraf et al., 2018).

Using a one-step KOH activation process, the research successfully produced hierarchical porous activated carbon from biowaste, which may be used as ultrahigh-

performance supercapacitor electrode material. The activated carbon (CSAC) that was made from coconut shells had a structure resembling a honeycomb and a high specific surface area of 2228 m^2/g along with a significant pore volume of 1.07 cm^3/g. The symmetric supercapacitor loaded with 6 M KOH had remarkable capacitance in its initial trials, measuring 367 F/g at 0.2 A/g. This capacitance was maintained for 10,000 cycles at 10 A/g. Additionally, a zinc-ion hybrid supercapacitor using CSAC as a cathode demonstrated outstanding energy density, cycle stability, and high-rate capability, demonstrating the potential of carbons produced from biowaste for high-end energy storage applications (Wang et al., 2023).

A study was conducted to evaluate the physical and chemical properties of activated carbon generated from coconut shells for the purpose of hydrogen adsorption. With an average crystalline size of 10.69 nm and a BET surface area of 51.7 m^2/g, the activated carbon was observed. Well-defined pores were shown by SEM and functional groups and π-π^* transitions were validated by FTIR and UV-Vis spectroscopy. The setup for the experiment successfully displayed ionic hydrogen storage in a modified polymer electrolyte fuel cell, confirming the ability of activated carbon to store hydrogen (Singla et al., 2024).

Coconut shells were utilized to create hierarchical activated carbons through hydrothermal, KOH-activation, and carbonization processes, with varying KOH to hydrochar ratios. The resulting carbon, coated on nickel foams, possessed a surface area of 1567 m^2/g, featuring micropores and mesopores. It exhibited impressive electrochemical performance, reaching a capacitance of 449 F/g at 1 A/g in a 6 M $LiNO_3$ aqueous solution. In solid-state symmetric supercapacitors, it achieved a specific capacitance of 88 F/g at 1 A/g and a high energy density of 48.9 Wh/kg at 1 kW/kg. This was attributed to its significant surface area, pore distribution, and suitable electrolyte, ensuring stability over 5000 cycles (Lee et al., 2021).

Two different supercapacitor designs were made using activated carbon derived from coconut shells. The outcomes of the tests proved that it might be a financially viable substitute for more expensive materials such as carbon nanotubes and activated carbon. With a 10% PVdF binder, the disk-shaped supercapacitor demonstrated the maximum specific capacitance at 70 F/g. The supercapacitor that was flat-laminated and with the

same binder exhibited the lowest equivalent series resistance (ESR), at 10.1 ohms. This study proposes sources of high ESR and discusses ways to reduce it (Ajina & Isa, 2010).

2.2 Research Gap

Significant progress has been achieved in the study of using coconut shells as precursors for activated carbon in supercapacitor applications. On the other hand, there is a significant study gap concerning the activation process optimization. Prior research has examined diverse activation techniques, including high-temperature heating in a muffle furnace and acid treatment afterward; however, little is known about other activation approaches. Preheating the coconut shells in an oven prior to acid treatment is one possible optimization strategy that could provide benefits like increased precursor reactivity and better control over the activation process. This alternate method uses less energy and is simpler to process, which could improve the final activated carbon's porosity and electrochemical performance. Also, there have been limited reports on the electrochemical utilization of activated carbon derived from coconut shells originating in Nepal. Therefore, more investigation is required.

CHAPTER-3

OBJECTIVES

3.1 General objective

The primary goal of this study is to produce and assess activated carbon obtained from agricultural waste byproducts. Following this, the emphasis lies on utilizing this prepared substance for energy harvesting and storage applications.

3.2 Specific objectives

The specific objectives of the present study are as follows:

- To prepare highly nanoporous activated carbon from locally available, coconut shells precursor.
- To activate coconut shell precursor chemically using phosphoric acid for the development of porosity by mixing coconut shell powder and phosphoric acid.
- To characterize as prepared carbon sample using various techniques such as SEM, FTIR, iodine number and methylene blue number and to determine the surface area by using the methylene blue adsorption method.
- To study the electrochemical properties of as prepared activated carbon using Cyclic Voltammetry (CV), Galvanostatic charge discharge (GCD) and Electrochemical impedance spectroscopy (EIS).

CHAPTER-4

MATERIALS AND METHODS

4.1 Instruments

The following instruments have been used throughout the work.

a) Grinder

A steel blade grinder was used for preparing the coconut shell powder.

b) Sieve

The sample that was powdered in the grinder was sieved using a 250μm pore size sieve.

c) Electronic balance

The sample and reagents were weighed out using Phoenix, PH2204C.

d) Hot air oven

For drying and heating of materials, a Eurolab hot air oven was used.

e) Tube Furnace

Activated carbon was prepared using a tube furnace of specification; KJ-T1200, AC220V single phase, 50Hz, max power 2kW, Serial no. KJLXR21120704, of ZHENGZHOU KEJIA FURNACE CO., LTD.

f) Sonicator

The DC-150H model of the MRC laboratory sonicator has been utilized to uniformly distribute the slurry.

g) Rotatory Flask Shaker

A rotatory flask shaker was employed to adsorb the material.

h) Filter Paper

Whatmann-1, 125μm, was used to filter.

i) Mortar and Pestle

The carbon was ground into a fine powder using mortar and pestle (COLE-PARMER INSTRUMENT 04010-00).

j) Field Emission Scanning Electron Microscopy (SEM)

ZEISS SEM Germany was utilized to examine the carbonized sample's surface morphology.

k) Fourier Transform Infrared Spectroscopy (FTIR)

Using an FTIR spectrophotometer (PerkinElmer 10.6.2), the surface functional groups of the carbon samples were investigated.

l) Potentiostat

CORRTEST (Wuhan, China) electrochemical workstation CS350H has been utilized for cyclic voltammetry, chronopotentiometry & electrochemical impedance spectroscopy.

m) Counter Electrode

Platinum wire was used as a counter electrode.

n) Reference Electrode

The Hg/HgO electrode was used as a reference electrode.

4.2 Chemicals

i. Phosphoric acid:

Fisher Scientific's Ortho Phosphoric Acid (H_3PO_4 88%) was purchased to activate the precursor.

ii. Potassium dichromate:

Potassium dichromate was obtained from SD Fine, India.

iii. Sodium thiosulphate:

Sodium thiosulphate was purchased from SD Fine, India.

iv. Hydrochloric acid:

LOBA CHEMIE PVT. LTD (35%) hydrochloric acid was used**.**

v. Sodium bicarbonate:

Fisher Scientific, India was the source of the sodium bicarbonate.

vi. Iodine:

Iodine was obtained from the Fisher Scientific, India.

vii. Potassium Iodide:

EMPLURA Potassium Iodide was used.

viii. Starch:

The starch solution from brought from Qualikems.

ix. Charcoal Activated - 250:

The Qualigens activated Charcoal was used.

x. **Ethanol (AR):**

Absolute ethanol was obtained from Changshu Hongsheng Fine Chemicals Co., Ltd.

xi. **Methylene Blue:**

The methylene blue was purchased from Merck company.

xii. **Isopropyl alcohol:**

Isopropyl alcohol was brought from Mount Everest Industrial Works.

4.3 Preparation of Reagents

4.3.1. Preparation of 0.1 N Sodium thiosulphate solution

In a 1000 mL volumetric flask, exactly 24.818 g of sodium thiosulphate was dissolved in distilled water and diluted to the appropriate level with distilled water to make the 0.1 N solution.

4.3.2. Preparation of 0.1 N $K_2Cr_2O_7$ solution

The 7.35 g of potassium dichromate crystal was weighed out accurately and dissolved in distilled water in a 250 mL volumetric flask, and the mixture was then diluted up to the mark with distilled water to prepare a 0.1 N solution of potassium dichromate.

4.3.3. Preparation of iodine solution

Firstly, 6.35 g of iodine crystal was exactly weighed out and dissolved in 25 mL of distilled water to prepare Solution A. Using 9.85 g of potassium iodide and 25 mL of distilled water, solution B was prepared. Next, 5 mL of solution A and 5 mL of solution B were mixed in a beaker while being constantly stirred to create an iodine solution with a 0.1 N concentration. After that, the mixture was let to remain for four hours to guarantee that the iodine crystal had completely dissolved. After the solution was transferred into a 500 mL volumetric flask, the appropriate amount of distilled water was added. Shaking the flask thoroughly ensured that the solution was uniform. To guarantee that the light radiation ceased, the solution was appropriately sealed off in the dark.

4.3.4. Preparation of starch solution

A slurry of starch solution was prepared by dissolving one gram of starch in 10 mL of distilled water. After then, 90 mL of boiling water was added to the mixture to make 100 mL. The solution was then allowed to cool to room temperature after boiling for five minutes.

4.3.5. Preparation of 5% HCl by weight

To prepare a 5% HCl solution by weight, 70 mL of concentrated HCl was mixed with 550 mL of distilled water.

4.3.6. Preparation of 10% Sodium bicarbonate ($NaHCO_3$)

In a 100 mL volumetric flask, sodium bicarbonate ($NaHCO_3$) weighing 10 g was placed, followed by the addition of 25 mL of distilled water. The flask was thoroughly shaken to ensure complete dissolution of the $NaHCO_3$, and then distilled water was added to fill it up to the mark.

4.3.7. Preparation of (2 M) KOH

To prepare (2 M) KOH solution in a 100 mL volumetric flask, 22.4 g of potassium hydroxide (KOH) pellets or flakes were dissolved in distilled water. The KOH was gradually added while stirring until fully dissolved. Once dissolved, the solution was diluted to the mark on the volumetric flask with distilled water. Then it was mixed thoroughly and stored in a labeled container.

4.3.8. Preparation of 500 ppm stock solution of methylene blue

Stock (500 mg/L) solution of methylene blue was prepared by dissolving 0.25 g of methylene blue in distilled water in a 500 mL volumetric flask. The working solutions of methylene blue of required concentrations were prepared by diluting the required volume of stock solution.

4.4 Preparation of Activated Carbon

4.4.1. Preparation of raw adsorbent from coconut shell

Coconut shells were collected from the local market of Kathmandu which were washed and sun-dried. Then, it was ground into fine powder using an electric grinder and sieved by using a 250 μm sieve. It was preheated for 2 hrs in an oven to eliminate moisture.

4.4.2. Preparation of chemical treated coconut shell powder

Thus, obtained coconut shell powder was treated with phosphoric acid (H_3PO_4) in a ratio 1:1 by weight and left for 24 hrs at room temperature. After 24 hrs, the sample was heated in a hot air oven for 2 hrs at 110 °C. Then, it was ground to fine powder using mortar and pestle.

4.4.3. Carbonization of Sample

The acid-treated sample was positioned in a ceramic combustion boat and placed into the tube furnace. Subsequently, the temperature of the furnace was raised gradually at a rate of 5 °C per minute. It underwent carbonization at 400 °C for 3 hrs using an inert nitrogen atmosphere, here pure nitrogen was supplied during the carbonization process. Following this, the carbonized sample was cooled to ambient temperature. Then, it was washed till neutral pH.

The carbon samples were labeled with names as outlined in **Table 1**.

Table 1: List of samples with their labels

S.N.	**Samples**	**Labeled names**
1.	Raw sample	CS-1
2.	Acid treated sample	CS-2
3.	Activated carbon	CS-3
4.	Commercial sample	CS

Table 2: Name of carbon samples with preparation conditions

Sample	**Particle size (μm)**	**Preheating temperature prior to activation (°C)**	**Preheating time (hr)**	**H_3PO_4: CSP ratio (wt:wt)**	**Heating temperature after chemical treatment (°C)**	**Heating time after chemical treatment (hr)**	**Carbonization temperature (°C)**	**Carbonization time (hr)**
CS-1	<250	200	2	-	-	-	-	-
CS-2	<250	200	2	1:1	110	2	-	-
CS-3	<250	200	2	1:1	110	2	400	3

4.5 Characterization

The surface morphology of the AC was studied by using SEM. Similarly, the surface functional groups were determined by using FTIR spectroscopy. The porosity developed in the AC was determined by using the methylene blue number and iodine number. The surface area was determined by using the methylene blue adsorption method. Also, CV, GCD and EIS were measured for electrochemical characterization.

4.5.1. Scanning Electron Microscopy (SEM)

SEM was operated at an accelerating voltage of 3.00 kV to study the surface morphology of as prepared carbon sample.

4.5.2. Fourier Transmission Infrared (FTIR)Spectroscopy

The FTIR spectra of as samples were recorded between 4000-500 cm^{-1} to study the presence of surface functional groups.

4.5.3. Iodine Number

4.5.3.1. Standardization of sodium thiosulphate

Sodium thiosulphate was standardized using a standard solution of 0.1 N $K_2Cr_2O_7$. Initially, 15 mL of water was placed in a 250 mL conical flask. Then, 15 mL of 10% KI and 10 mL of 10% $NaHCO_3$ were added and thoroughly mixed. Following this, 3 mL of concentrated HCl was slowly added and gently mixed. Subsequently, 25 mL of 0.1 N $K_2Cr_2O_7$ solution was added, and the flask's sides were rinsed with a small amount of water. The mixture was covered with a watch glass, shaken well, and left in the dark for approximately 5 minutes. The watch glass and inner walls of the flask were rinsed with distilled water to capture any vaporized iodine in the solution. The solution was then titrated against sodium thiosulfate solution with continuous shaking until a yellowish-green color appeared. Around 1 mL of freshly prepared starch solution was added, resulting in a blue color. With the continuous addition of sodium thiosulfate solution, the color changed from blue to light green. The volume of thiosulfate consumed was recorded, and its concentration was subsequently calculated.

4.5.3.2. Standardization of iodine solution

Prior to determining the iodine number, the iodine solution was standardized using a standard solution of sodium thiosulfate. Initially, 25 mL of the iodine solution was measured and transferred into a 250 mL conical flask. It was then subjected to titration with standardized sodium thiosulfate solution until the iodine solution turned a light yellow color. A few drops of the starch indicator were added, and titration proceeded drop by drop until a colorless solution was observed. The volume of thiosulfate solution from the burette was recorded, and the concentration of iodine was calculated.

4.5.3.3. Determination of iodine number

In a conical flask, 0.1 g of activated carbon (AC) was placed, followed by the addition of 5 mL of 5% HCl, which was then heated to boiling and allowed to cool.

Subsequently, 10 mL of 0.1 N iodine solution was introduced into the flask, and the mixture was vigorously shaken in a mechanical shaker for 15 minutes. Afterward, it was filtered and the filtrate was titrated with standard thiosulphate solution using starch as an indicator. This process was repeated three times consecutively. The quantity of thiosulphate consumed was measured, and the iodine number was then calculated.

4.5.4. Determination of methylene blue number

4.5.4.1. Determination of λ_{max} for methylene blue (MB)

Dilutions were prepared from the stock solution to obtain concentrations of 100 mg/L and 10 mg/L. Using a serial dilution technique, further dilutions were carried out to produce a range of concentrations from 1 to 9 mg/L. The absorbance of a 5 mg/L solution was then assessed using a UV spectrophotometer to identify the maximum absorbance (λ_{max}) associated with the concentration of methylene blue, which was plotted on a graph.

4.5.4.2. Determination of MB number

In a conical flask, 50 mL of a 100 mg/L methylene blue (MB) solution was accurately measured, and 0.025 g of prepared activated carbon (AC) was added. The mixture was vigorously shaken to ensure thorough dispersion. Next, it was placed in a Rotatory Flask Shaker for 5 hours at 200 rpm to aid the adsorption process. Subsequently, the solution was allowed to settle for 24 hours, after which it was filtered. The absorbance of the MB solution was then determined using a UV Spectrophotometer at its maximum wavelength (λ_{max}). Finally, the concentration of MB was calculated using the formula derived from the **equation (3) and (4)**.

4.5.5. Determination of specific surface area of prepared AC

To determine the surface area of as prepared AC, the Langmuir adsorption isotherm model was utilized, focusing on methylene blue (MB) adsorption.

For the MB adsorption process, the initial step involved obtaining the λ_{max} and calibration curve. Different concentrations of methylene blue solutions ranging from 1 to 10 mg/L were prepared by diluting a stock 500 mg/L MB solution in different 100 mL volumetric flasks. The λ_{max} was then measured within a wavelength range of 400 to 700 nm using a UV Spectrophotometer. The absorbance of each solution was recorded at the maximum wavelength to construct a calibration curve, enabling the determination of equilibrium concentration for the methylene blue solution.

To assess the surface area of the coconut shell material, the batch adsorption method was utilized. Initially, 25 mg of the prepared coconut shell-derived AC was accurately weighed and transferred into adsorption bottles containing methylene blue solutions of varying concentrations: 25 mg/L, 50 mg/L, 100 mg/L, 150 mg/L, 200 mg/L, and 250 mg/L.

These solutions were then agitated for 5 hrs in a mechanical shaker at 220 rpm. Subsequently, they were allowed to settle to obtain the supernatant solution, and the adsorbent material was removed. The absorbance of the resulting solution was noted at the maximum wavelength. The Langmuir isotherm was then plotted using equilibrium concentration/equilibrium adsorption as a function of equilibrium concentration. From this isotherm, the Q_m value was calculated, and the specific surface area of the prepared coconut shell-derived AC was determined using **equation (5)**.

4.5.6. Electrochemical Characterization of prepared AC

Electrochemical tests were conducted within a three-electrode setup, with the as-prepared activated carbon serving as the working electrode, Platinum (Pt) wire as the counter electrode, and Hg/HgO as the reference electrode. A 2 M solution of KOH was used as the electrolyte. The working electrode was prepared in the laboratory by combining the prepared AC, PVdF (binder), and commercial activated carbon in an 8:1:1 ratio. This mixture was ground in a mortar and pestle with the gradual addition of isopropyl alcohol. Afterward, it was transferred to a clean vial and sonicated for 15 minutes. Pure Ni foam was weighed, and the sonicated solution was applied to it using a drop-casting method. The coated foam was then dried in an oven at 60 °C for 10 minutes, with the process repeated until the solution was completely applied. Finally, the electrode was dried at 60 °C for 12 hours. Cyclic voltammetry and chronopotentiometry measurements were conducted within a potential range of 0 to 0.8 V using an Electrochemical Analyzer and EIS was also measured. The specific capacitance (C_{sp}) was determined from the discharge curve using **equation (9).**

The overall experimental processes are shown in flow chart diagram:

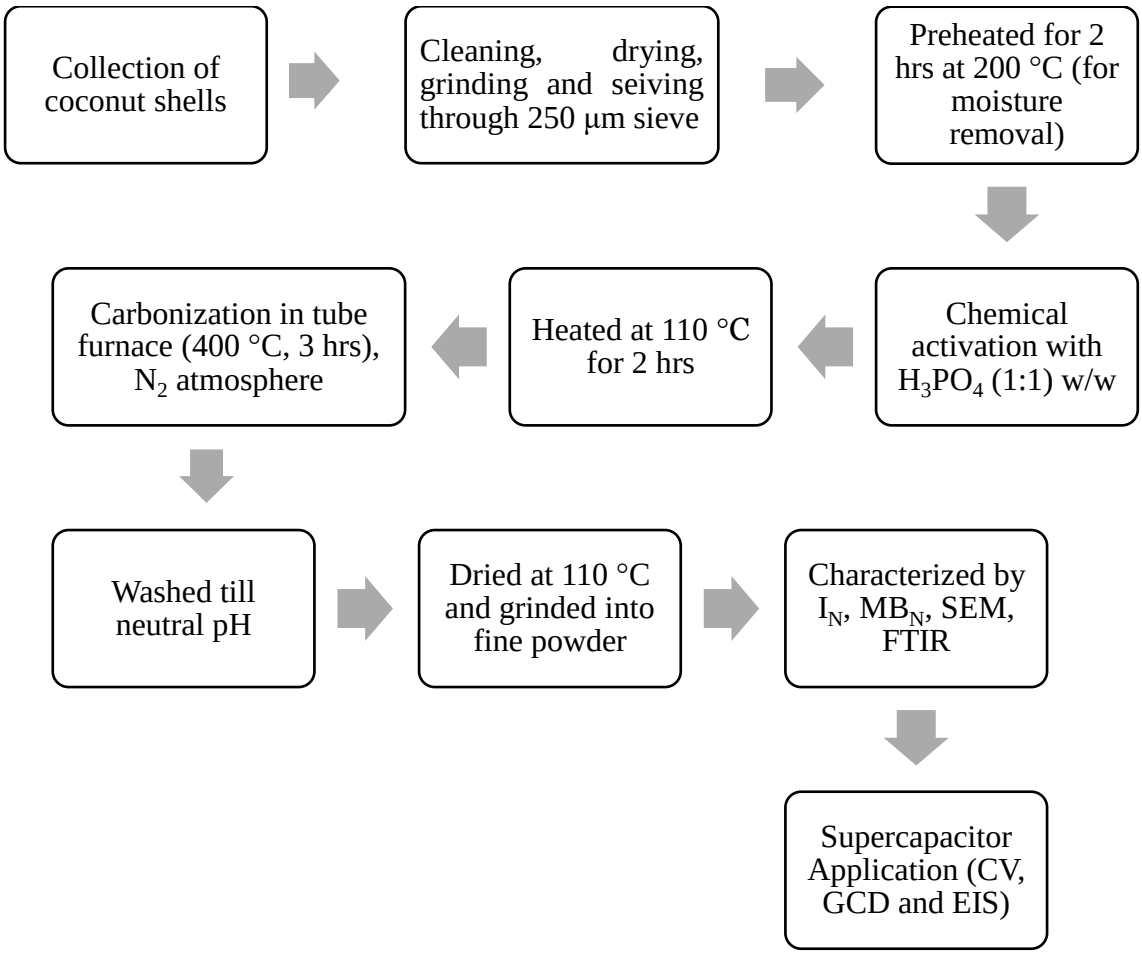

Figure 6: Flowchart diagram for the overall process of the experiment

CHAPTER-5

RESULTS AND DISCUSSION

5.1 Yield of activated carbon

The yield of activated carbon has been obtained by taking the ratio between the weight of the resulting activated carbon after activation and the initial mass of the raw materials prior to carbonization. The total yield obtained was 2.87 g when 5 g of precursor was carbonized, which was 57.4%. Thus, obtained AC was found to be black in colour with solid amorphous mass and is shown in **Fig. 7**.

Figure 7: Digital picture of laboratory prepared Activated carbon (AC)

5.2 Characterization of as prepared AC

5.2.1. Investigation of Surface morphology: SEM analysis

The SEM image of as prepared AC (CS-3) is shown in **Fig. 8**. **Figure 8 (a)** shows the SEM image in 100 µm magnification while **(b)** is a magnified SEM image in 10 µm. In the image, one can clearly see the presence of abundant pores varying in size and distribution. It also depicts the layered and rough structure along with the presence of cracks on the surface.

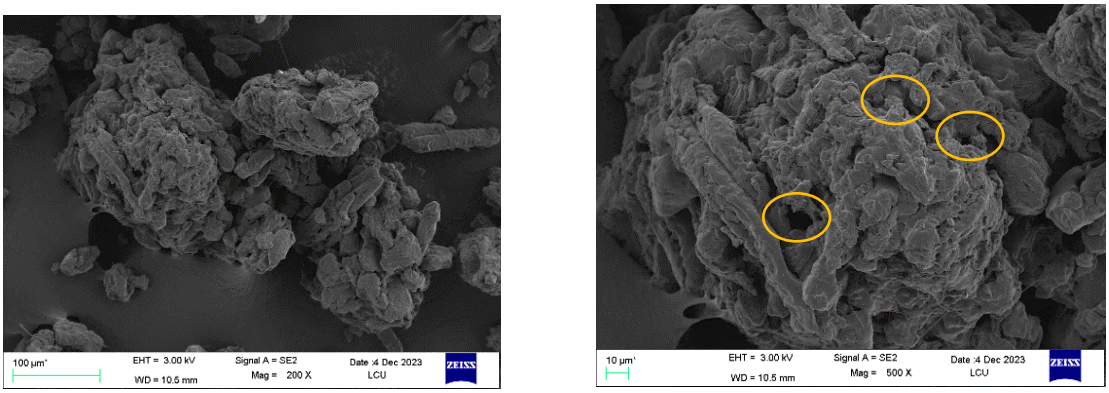

(a) **(b)**

Figure 8: SEM images of as prepared AC where **(a)** is in 100 µm and **(b)** is in 10 µm magnification

Such pores may be obtained due to the initial treatment of the precursor material with phosphoric acid. Phosphoric acid acts as a pore-forming agent, selectively removing

elements from the precursor and creating voids and channels within the material. Subsequent carbonization of the phosphoric acid-treated precursor at 400 °C further refines the porous structure of the activated carbon. During carbonization, the precursor undergoes thermal decomposition and pyrolysis, resulting in the formation of a carbonaceous matrix with a network of interconnected pores. The moderate carbonization temperature ensures the preservation of the pore structure while imparting thermal stability to the material.

Here, the combined effect of phosphoric acid treatment as well as carbonization at 400 °C resulted in the formation of a porous carbon structure with a high surface area, making it suitable for energy applications.

5.2.2. Investigation of Oxygenated surface functional group: FTIR analysis

The surface functional groups in CS-1, CS-2 and CS-3 were analyzed by FTIR. The obtained spectra of CS-1 is shown in **Fig. 9**.

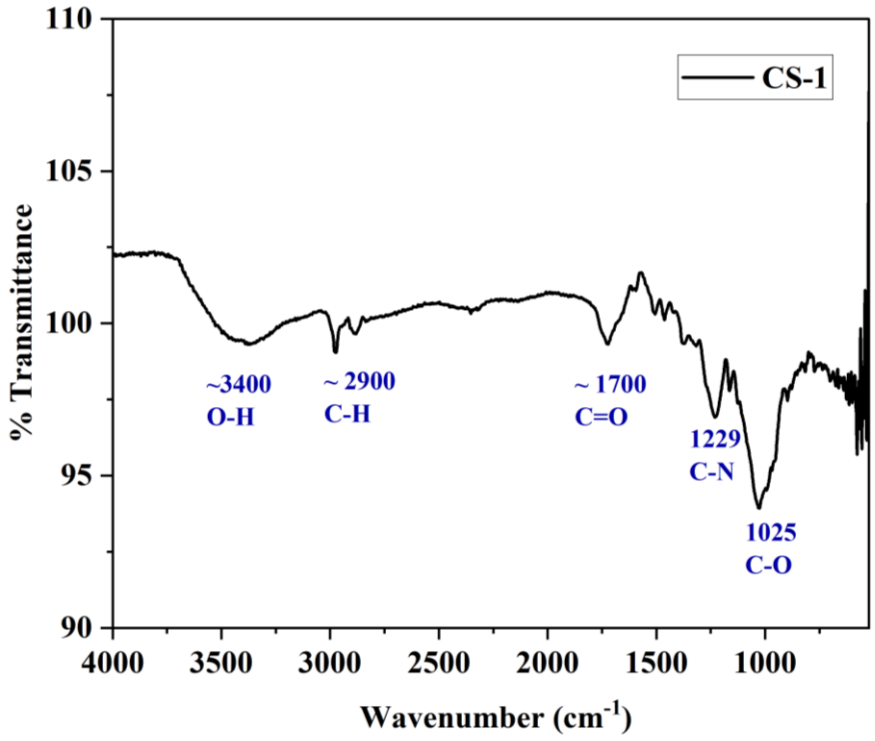

Figure 9: FTIR spectra of CS-1(Raw sample)

In **Fig. 9**, CS-1 represents the spectra of the raw sample where different bands are clearly seen at different wave numbers such as ~3400 cm^{-1}, ~2900 cm^{-1}, ~1700 cm^{-1} and so on. The band at around 3400 cm^{-1} indicates the O-H stretching vibration. Similarly, the band ~ 2900 cm^{-1} is assigned to C-H stretching vibration. Also, the band

~ 1700 cm^{-1} indicates the C=O stretching vibration of carbonyl groups. Bands at 1229 cm^{-1} & 1025 cm^{-1} were also seen which are associated with C-N stretching vibration of the amine group and C-O stretching vibration in the ether group respectively.

The obtained spectra of CS-2 is shown in **Fig. 10**.

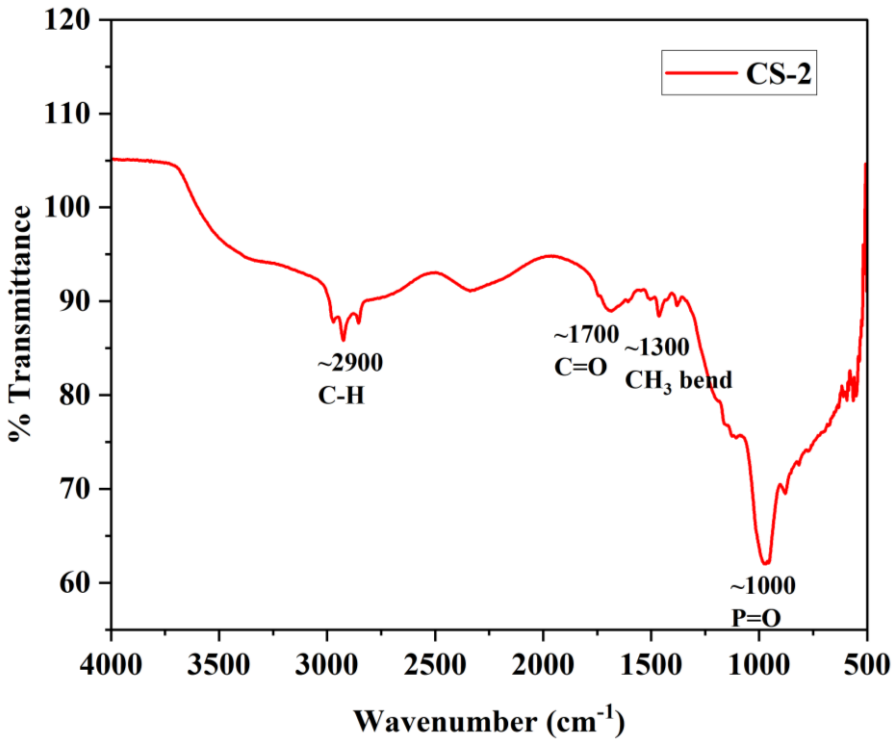

Figure 10: FTIR spectra of CS-2 (acid treated sample)

In **Fig. 10**, CS-2 represents the acid treated sample where one can see the band at ~ 2900 cm^{-1} which is the C-H stretching vibration of aliphatic hydrocarbons. Also, the band ~ 1700 cm^{-1} is seen that is assigned to C=O of carbonyl groups. Similarly, ~ 1300 cm^{-1} CH_3 bending vibration is seen. A distinct band is also seen ~ 1000 cm^{-1} which is the P=O stretching vibration of a phosphate group.

The obtained spectra of CS-3 is shown in **Fig. 11**.

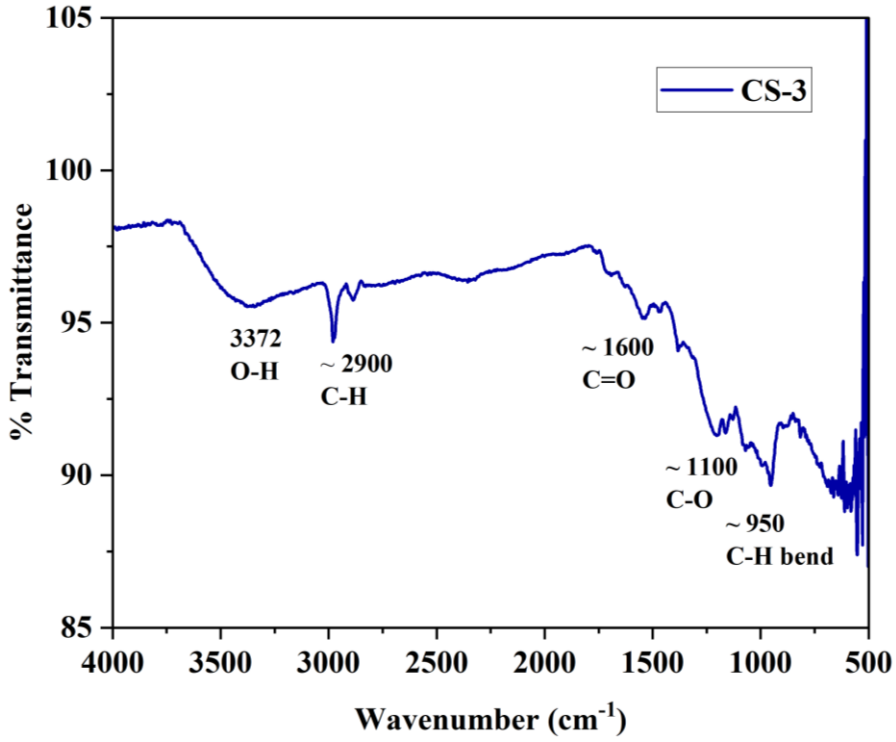

Figure 11: FTIR spectra of CS-3 (activated carbon)

In the same way, **Fig. 11** represents the spectra of CS-3 which is as prepared activated carbon. Here, one can clearly see the band at 3272 cm^{-1} which is the O-H stretching vibration of a phenolic or alcoholic group. Another band at ~ 2900 cm^{-1} represents the C-H stretching vibration of alkane. Similarly, the band at ~ 1600 cm^{-1} is clearly perceived which is assigned for C=O stretching vibration of carbonyl groups. One can see a band around 1100 cm^{-1} which is C-O stretching vibration. Also, the band seen at ~ 950 cm^{-1} is the C-H bending vibration of the aromatic group.

The spectral analysis revealed that a sufficient amount of surface functionality has been developed at the surface of as prepared material. These oxygenated surface functional groups affect the wettability, hydrophilicity, surface accessibility to aqueous electrolytes in activated carbon which will help to increase which increases the electrical conductivity.

5.2.3. Investigation of microporosity: Iodine number (I_N) method

The iodine number indicates the presence of micropores in activated carbon. In this study, the iodine numbers of the raw sample, acid-treated sample, activated carbon, and commercial sample were investigated. The results presented in **Table 3** display the iodine numbers obtained for the samples. The findings indicate that the commercial sample exhibited the highest iodine number, suggesting adequate microporosity. Similarly, in as prepared AC sample (CS-3) 821.7 mg/g I_N value was obtained indicating plenty of microporosity than in CS-2 and CS-1. Porosity development may be due to chemical activation and carbonization.

Table 3: Iodine number of as prepared carbon samples

S.N	Sample	Iodine number (mg/g)
1.	Raw sample (CS-1)	406.4
2.	Acid Treated (CS-2)	520.7
3.	Activated Carbon (CS-3)	821.7
4.	Commercial Sample (CS)	1016.0

5.2.4. Investigation of Mesoporosity: Methylene blue number (MB_N) method

The absorbance of MB as a function of wavelength is shown in **Fig. 12**. The maximum absorbance was obtained at 665 nm which is used as the maximum wavelength λ_{max} for the entire work.

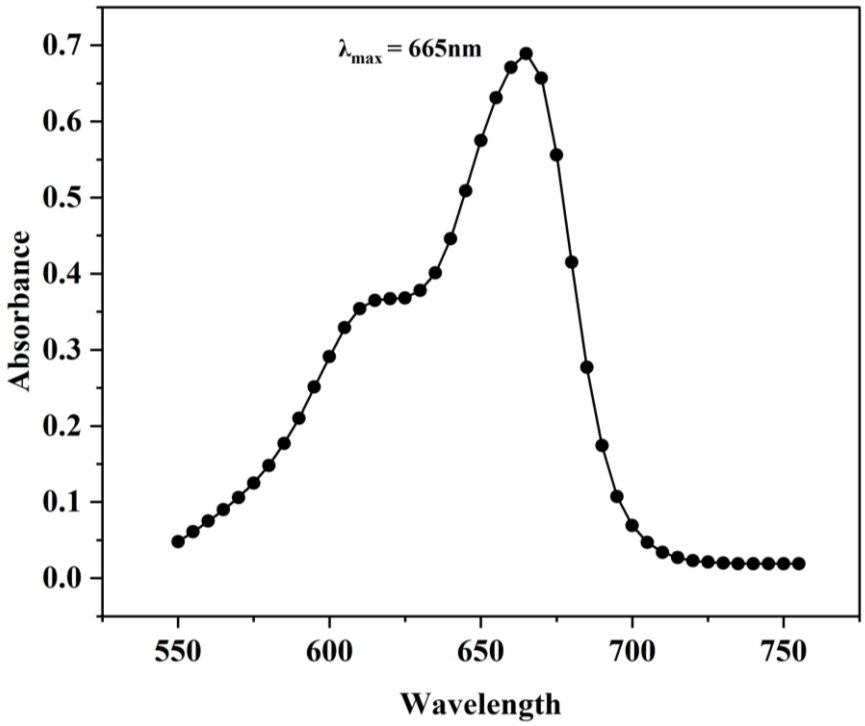

Figure 12: A plot of absorbance as a function of wavelength

The calibration curve of methylene blue solution is shown in **Fig. 13**. It shows the relation between absorbance and concentration following Beer Lambert's law.

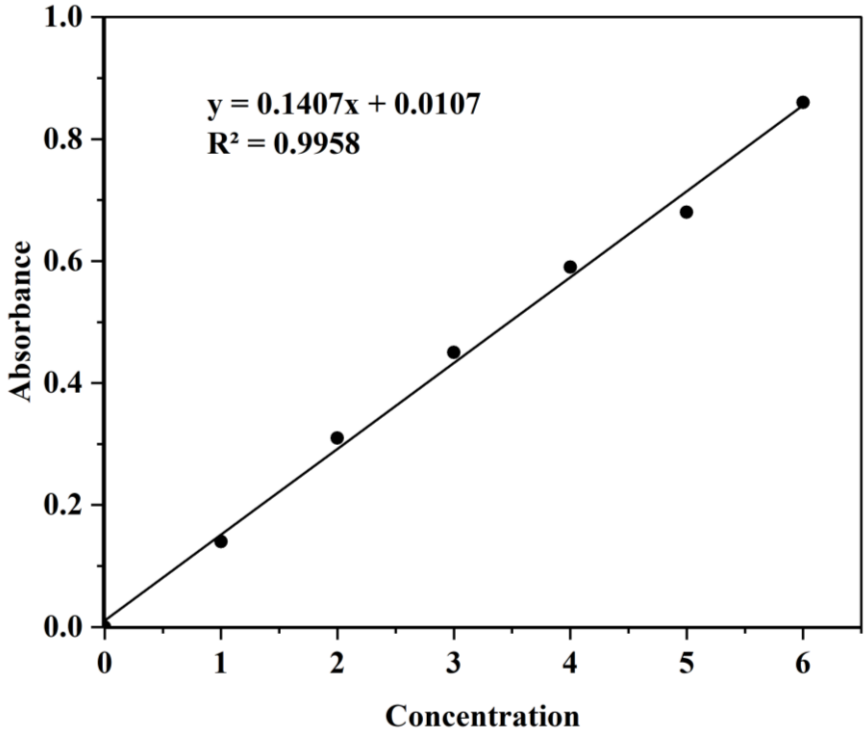

Figure 13: Calibration curve for the determination of MB

The MB_N of prepared activated carbon (CS-3) was found to be 181.52 mg/g calculated using **equation 3**. It indicates the presence of mesopores on the activated carbon surface (Bestani et al., 2008). The porosity may be created due to chemical activation and carbonization. It is presumed that bottleneck pores and micro to mesopores were improved by developing oxygenated surface functional groups as indicated by FTIR (**Fig.11**). The process began with treating the material with phosphoric acid at room temperature. Following this, heat treatment was applied, which removed some of the surface functional groups. This caused the closed pores and bottleneck pores to broaden and mesoporosity was transpired.

5.2.5. Determination of specific surface area: MB adsorption method (Brina & Battisti., 1987)

The Langmuir curve is shown in **Fig. 14** which is used to determine the specific surface area.

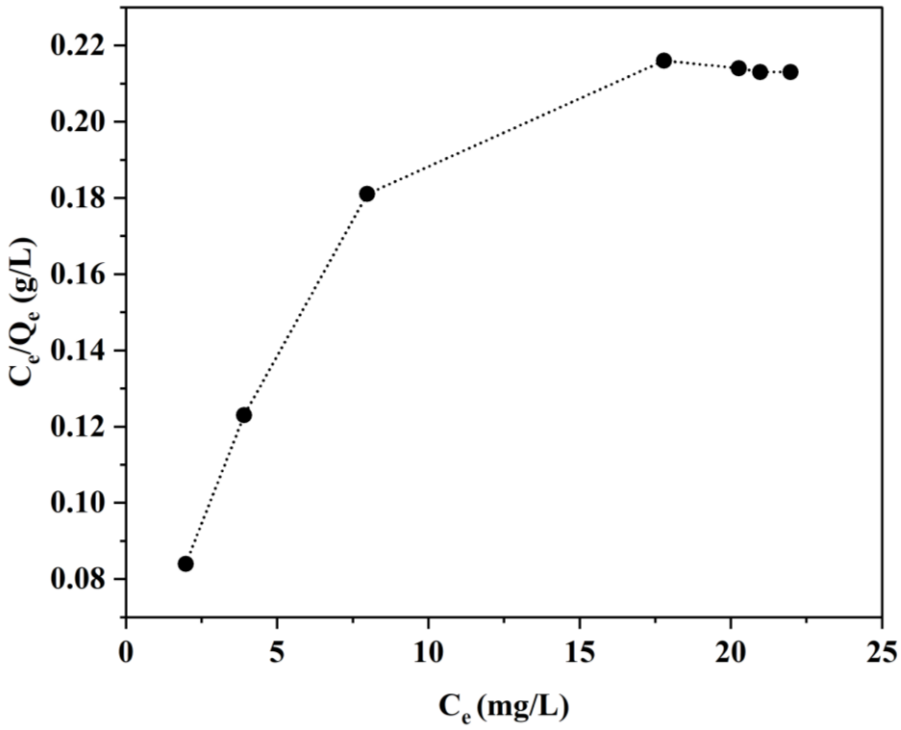

Figure 14: Curve showing C_e/Q_e as a function of C_e

The corresponding Langmuir parameters were obtained and the specific surface area was calculated by using the formula (**equation 5**). The specific surface area of the CS-3 sample was found to be 802.12 m^2/g. The high surface area of the as prepared activated carbon may be due to the presence of the abundant number of pores varying in sizes which is confirmed by SEM, I_N and MB_N.

5.3 Electrochemical characterization

5.3.1. Cyclic Voltammetry

The cyclic voltammetry (CV) analysis of the sample across different scan rates reveals its remarkable capacitive behavior and electrochemical performance. The analysis involved examining cyclic voltammograms, as shown in **Fig. 15**, which depict the material's behavior under different scan rates (10, 20, 50, 80, and 100 mV/s).

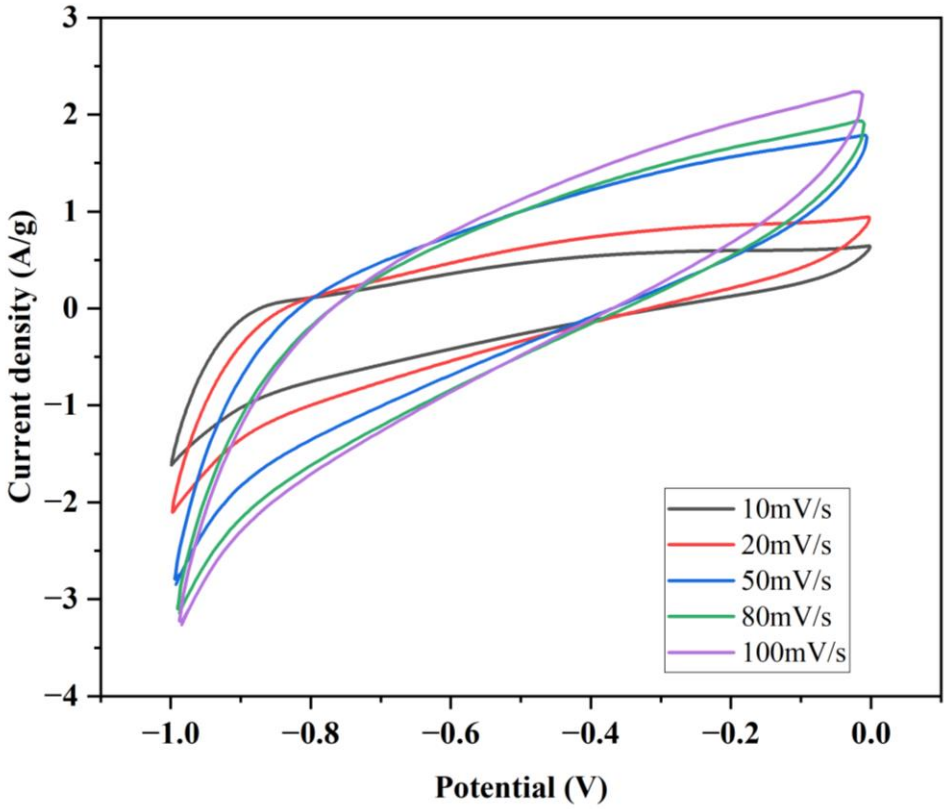

Figure 15: Cyclic voltammogram of activated carbon (CS-3) at different scan rates

Fig. 15 shows the consistently rectangular shape of the CV curves, coupled with their symmetrical nature, indicating the material's high reversibility and adherence to ideal electrical double-layer capacitor (EDLC) behavior. It may be due to contribution of oxygenated surface functional groups. However, deviations from the ideal rectangular shape may occur due to factors like migration forces and polarized resistance, which impede electrolyte ion diffusion. As the scan rate increases, the peak current responses also rise, reflecting the material's ability to facilitate faster charging and discharging processes. This behavior emphasizes its suitability for applications requiring rapid energy storage and release. Moreover, the absence of distinct redox peaks suggests that

the charge storage mechanism primarily involves electrostatic interactions at the electrode-electrolyte interface, emphasizing its capacitive nature.

Overall, the sample demonstrates excellent electrochemical characteristics, including high reversibility, rapid ion diffusion kinetics, and ideal capacitive behavior, positioning it as a promising candidate for various energy storage applications, such as supercapacitors, where efficient and rapid charge storage is essential.

The current response of activated carbon (CS-3) at different scan rates is given in **Table 4**.

Table 4: Table showing the current response of CS-3 at various scan rates

Scan rates (mV/s)	Current response (A/g)
10	0.61
20	0.93
50	1.77
80	1.91
100	2.23

The highest current response of 2.23 A was obtained when 100 mV potential was applied and the least was found to be 0.61 A at 10 mV/s scan rate. Higher scan rates typically lead to higher current responses which may be due to enhanced mass transport, faster electrochemical kinetics, increased double layer capacitance, and polarization effects.

5.3.2. Chronopotentiometry

Chronopotentiometry was employed to conduct charge-discharge measurements, evaluating the electrochemical characteristics of as prepared activated carbon derived from coconut shells (CS-3). The Galvanic Current Density (GCD) curve of activated carbon offers valuable insights into its electrochemical behavior, particularly in the context of energy harvesting and storage applications. The experiment involved testing the material within a potential range of 0 to -1 V against a Hg/HgO reference electrode, employing various current densities. By considering the total electrode mass, the charge-discharge current density was determined. Lower current densities led to slower discharge times.

Fig. 16 shows the typical GCD curves at different currents, i.e., 1-10 mA current was applied. One can see, that the charge discharge rate was found to be highest at the current value of 1mA and the current density was found to be 0.33 A/g. Here, the charging time is faster whereas the discharging time is slower. The discharge time was found to be 409.25 s which is relatively higher than the value found in literature (Shrestha et al., 2021) whereas the charging time is only 139.6 s. Curves are almost symmetrical which indicates the reversibility of the electrode as well as double layer capacitive behavior.

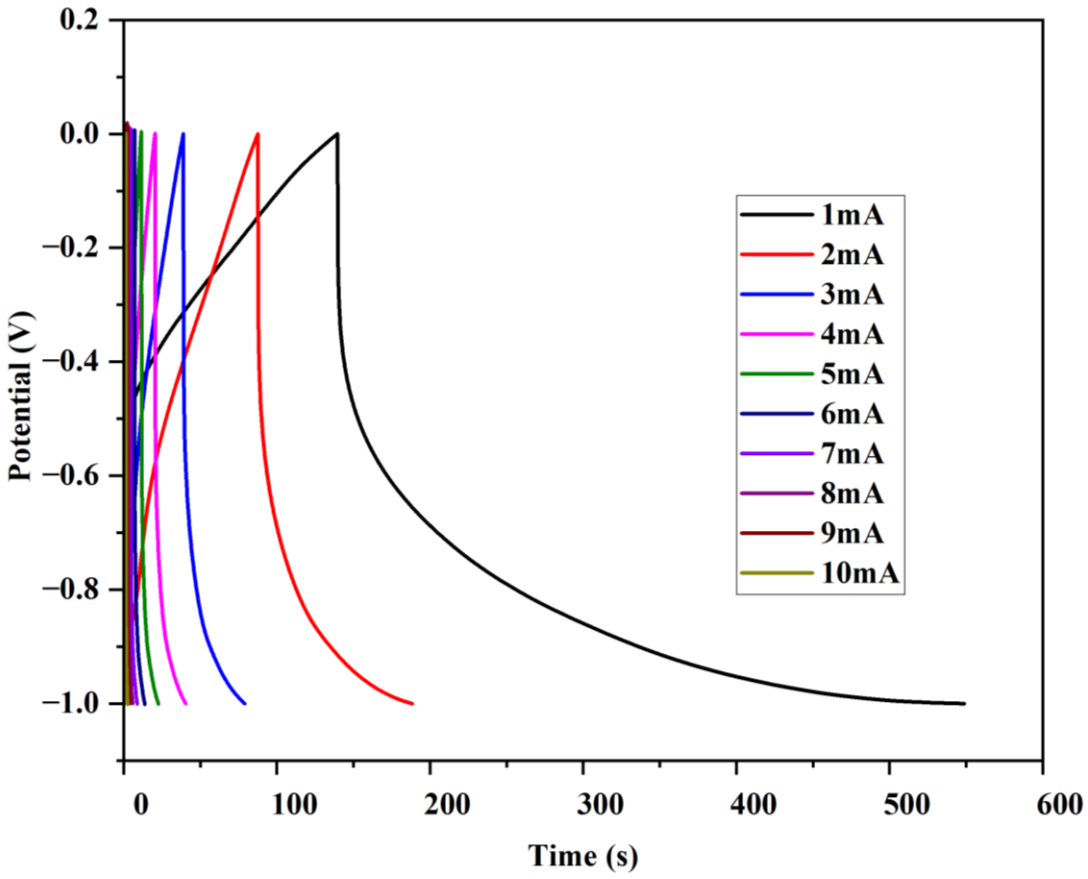

Figure 16: GCD curve of CS-3 at different current

The specific capacitance (C_{sp}) in 1 mA current was also calculated and was found to be the highest which is 136.42 F/g and its current density was found to be 0.3 A/g. Similarly, the C_{sp} at current densities of 0.6 A/g and 1 A/g were also calculated using **equation (9)** which is presented in **Table 5**.

Table 5: Specific Capacitance of AC at different current densities

Sample Name	Current density (A/g)	Specific Capacitance (F/g)
CS-3	0.3	136.42
	0.6	67.58
	1	40.25
	1.3	27.06
	1.6	18.47

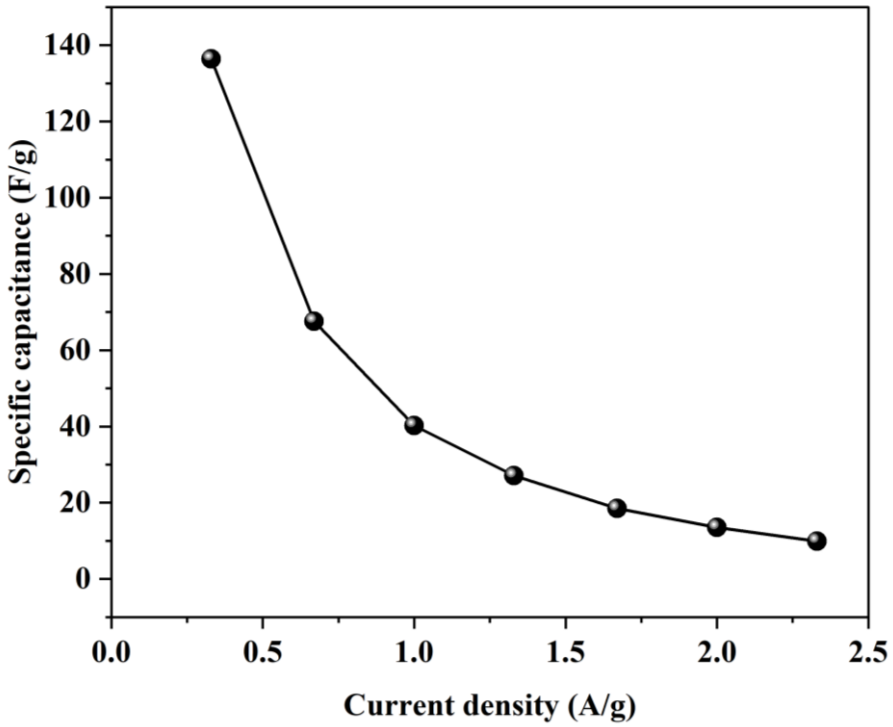

Figure 17: Specific capacitance as a function of current density

The graph shown in **Fig. 17** depicts the relationship between specific capacitance and current density for a given electrochemical system. Initially, at a low current density of 0.3 A/g, the specific capacitance is at its peak, 136 F/g. This high value indicates that the material efficiently stores charge when the current density is low. As the current density increases, there is a noticeable decline in specific capacitance. By 0.6 A/g, the specific capacitance has dropped significantly to 67 F/g. This trend continues, with specific capacitance decreasing to 40 F/g at 1.0 A/g and further to 27 F/g at 1.3 A/g. At 2.0 A/g, the specific capacitance reaches about 13 F/g, and finally reaches to around 10 F/g at the highest current density of 2.3 A/g.

This inverse relationship suggests that higher current densities lead to lower specific capacitance values. This phenomenon occurs because, at higher current densities, the time available for ions to diffuse and interact with the electrode material is reduced, resulting in less efficient charge storage. Additionally, increased internal resistance and kinetic limitations at higher current densities contribute to the decline in specific capacitance.

Then, further energy and power densities were also calculated using **equations (10) and (11)** respectively which are given in **Table 6**.

Table 6: Specific capacitance, Energy density and Power density value of CS-3 sample

Sample Name	Specific Capacitance (F/g)	Energy density (Wh/kg)	Power density (W/kg)
CS-3	136.42	68.21	600

The high C_{sp}, E_d and P_d may be due to the porous structure as indicated by SEM image (**Fig. 8**) and high surface area of the as prepared activated carbon. The surface functionality (**Fig. 11**) also improved electrolyte wettability, hydrophilicity, surface accessibility to aqueous electrolytes in AC material which ultimately improved the charge discharge rate and allows one to achieve higher specific conductance. The C_{sp} and E_d values were relatively better than the literature (Lee et al., 2021). The obtained E_d value is significantly higher than that of a typical supercapacitor.

5.3.3. Electrochemical Impedance Spectroscopy (EIS)

It is the method employed for investigating the resistance in supercapacitors which involves analyzing the electrochemical processes occurring at different time scales through current responses across a range of frequencies. This approach allows for distinguishing between electronic and ionic processes. In **Fig. 18**, the Nyquist impedance plot of the as-prepared activated carbon (CS-3) electrode in a 0.2 M KOH electrolyte, is presented. The data points represent experimental observations. The semicircle curve is associated with polarization resistance, which signifies the diffusion or transport of electrolytes into the porous electrode material (Shrestha et al., 2019). Two capacitive loops are evident in the plot: one at the lower frequency region and the other at the higher frequency region. The smaller loop corresponds to diffusion

impedance in parallel with double-layer capacitance, while the larger loop represents charge transfer resistance along with double-layer capacitance.

In **Fig. 18**, it was observed that the Equivalent Series Resistance (ESR) value was remarkably low, measuring 2.1 Ω. This indicates minimal resistance during current transfer, compared to the literature value of 10.1 Ω (Ajina & Isa, 2010).

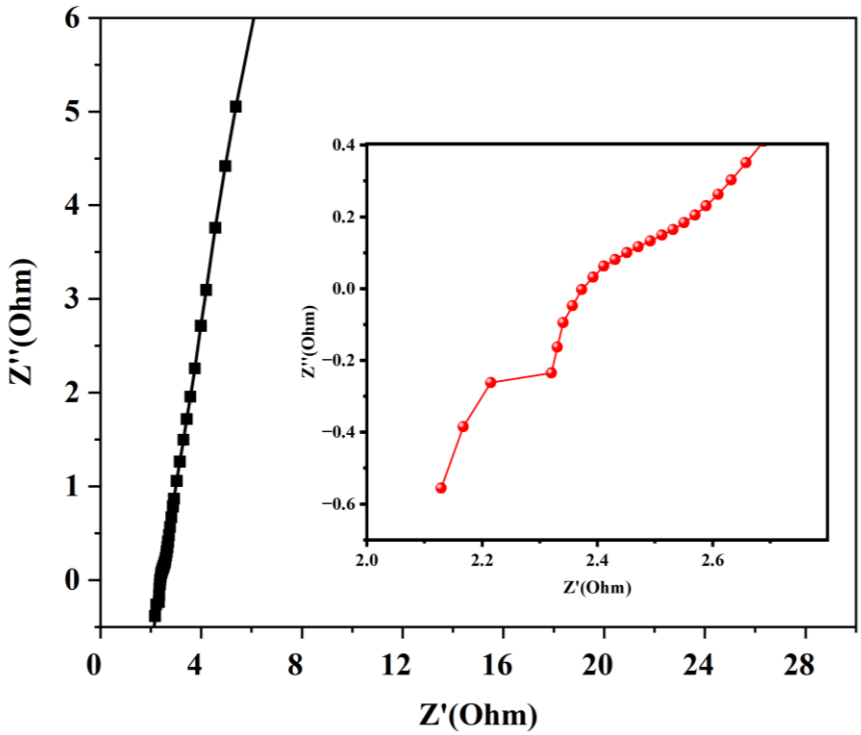

Figure 18: Nyquist plot obtained in CS-3 sample. The enlarged plot is shown in the inset picture.

CHAPTER-6

CONCLUSION

The study investigated the utilization of activated carbon obtained from waste coconut shells for supercapacitor applications. The activation process involved treating coconut shell powder with phosphoric acid, followed by thermal treatment in an inert atmosphere using a tube furnace. The carbonization process resulted in a yield of 57.4% carbon. The resulting activated carbon was characterized through various analytical methods such as methylene blue number, iodine number, surface area determination, FTIR, SEM and electrochemical characterization.

The iodine number, of the raw sample, acid treated sample, activated carbon and commercial carbon was found to be 406.4, 520.7, 821.7 and 1016 mg/g respectively which indicates the development of micropores in as prepared AC. The mesoporosity of the activated carbon was assessed using the methylene blue number method, resulting in a value of 181.52 mg/g. Likewise, the specific surface area was determined through methylene blue adsorption, yielding a measurement of 802.12 m^2/g.

The SEM image shows a rough, porous structure, indicating the development of porosity during activation. FTIR spectra confirmed the presence of oxygenated functional groups such as hydroxyl, carbonyl and carboxyl on the surface of AC.

The symmetrical rectangular cyclic voltammetry curve confirms the electric double-layer capacitor (EDLC) behavior, resulting in a specific capacitance of 136.42 F/g at a current density of 0.3 A/g. Energy density was found to be 68.21 Wh/kg which is significantly higher than in a typical supercapacitor (2-8 Wh/kg) and power density was found to be 600 W/kg which aligns with the value of P_d of a typical supercapacitor.

Bottleneck pores and micro to mesopores were improved by developing oxygenated surface functional groups. The process began with treating the material with phosphoric acid at room temperature. Following this, heat treatment was applied, which removed some of the surface functional groups. This caused the closed pores and bottleneck pores to broaden, facilitating charge migration into the pores. Consequently, the specific capacitance increased, leading to a faster frequency response and better ion transport. These modifications ultimately enhanced the material's power storage

characteristics. These findings suggest that activated carbon derived from coconut shells is effective as an electrode material in supercapacitor devices.

FUTURE PROSPECTIVES

Further research can be done to see the effect of carbonization temperature on electrochemical characterization. Also, other activating agents like KOH, NaOH, $ZnCl_2$, etc can be used for comparative study. Further the ratio of activation can also be varied for optimization. Also, one can prepare the composite materials using coconut shell derived activated carbon for the enhancement in the specific conductance and overall supercapacitive performance.

REFERENCES

Abd, A. A., Naji, S. Z., Hashim, A. S., & Othman, M. R. (2020). Carbon dioxide removal through physical adsorption using carbonaceous and non-carbonaceous adsorbents: a review. Journal of Environmental Chemical Engineering, 8(5), 104142

Abdel Maksoud, M. I. A., Fahim, R. A., Shalan, A. E., Abd Elkodous, M., Olojede, S. O., Osman, A. I., ... & Rooney, D. W. (2021). Advanced materials and technologies for supercapacitors used in energy conversion and storage: a review. Environmental Chemistry Letters, 19, 375-439.

Abdullah, A., & Mohammed, A. (2019, November). Scanning electron microscopy (SEM): A review. In Proceedings of 2018 International Conference on Hydraulics and Pneumatics-HERVEX, 77-85.

Adan-Mas, A., Alcaraz, L., Arévalo-Cid, P., López-Gómez, F. A., & Montemor, F. (2021). Coffee-derived activated carbon from second biowaste for supercapacitor applications. Waste Management, 120, 280-289.

Agbozu, I. E., & Emoruwa, F. O. (2014). Batch adsorption of heavy metals (Cu, Pb, Fe, Cr and Cd) from aqueous solutions using coconut husk. African Journal of Environmental Science and Technology, 8(4), 239-246.

Ajina, A., & Isa, D. (2010). Symmetrical supercapacitor using coconut shell-based activated carbon. Pertanika J. Sci. Technol, 18, 351-363.

Akpro, L. A., Gbogouri, G. A., Konan, B. R., Issali, A. E., Konan, K. J. L., Brou, K. D., & Nemlin, G. J. (2019). Phytochemical compounds, antioxidant activity and non-enzymatic browning of sugars extracted from the water of immature coconut (Cocos nucifera L.). Scientific African, 6, e00123.

Ali, S. N., El-Shafey, E. I., Al-Busafi, S., & Al-Lawati, H. A. (2019). Adsorption of chlorpheniramine and ibuprofen on surface functionalized activated carbons from deionized water and spiked hospital wastewater. Journal of environmental chemical engineering, 7(1), 102860.

Ashraf, C. M., Anilkumar, K. M., Jinisha, B., Manoj, M., Pradeep, V. S., & Jayalekshmi, S. (2018). Acid washed, steam activated, coconut shell derived

carbon for high power supercapacitor applications. Journal of The Electrochemical Society, 165(5), A900.

Aygün, A., Yenisoy-Karakaş, S., & Duman, I. (2003). Production of granular activated carbon from fruit stones and nutshells and evaluation of their physical, chemical and adsorption properties. Microporous and mesoporous materials, 66(2-3), 189-195.

Banu, S. A., Nagarani, S., & Kirubha, M. (2016). Preparation of Low Cost Activated Carbon Adsorbents from Natural Sources. Int. J. Eng. Tech. Sci. & Re, 3(4), 43-46.

Bestani, B., Benderdouche, N., Benstaali, B., Belhakem, M., & Addou, A. (2008). Methylene blue and iodine adsorption onto an activated desert plant. Bioresource technology, 99(17), 8441-8444.

Bhoyate, S., Kahol, P. K., & Gupta, R. K. (2018). Nanostructured materials for supercapacitor applications. SPR Nanoscience, 05(02), 1–29.

Bottu, M., Crow, M. L., Elmore, A. C., & Atcitty, S. (2013). A Power electronic conditioner using ultracapacitors to improve wind turbine power quality. Smart Grid and Renewable Energy, 04(01), 69–75.

Boukoussa, B., Cherdouane, K. R., Zegai, R., Mokhtar, A., Hachemaoui, M., Issam, I., ... & Abboud, M. (2024). Preparation of activated carbon-metal nanoparticle composite materials for the catalytic reduction of organic pollutants. Surfaces and Interfaces, 44, 103-622.

Brina, R., & De Battisti, A. (1987). Determination of the specific surface area of solids by means of adsorption data. Journal of Chemical Education, 64(2), 175.

Chang, C. K., Tun, H., & Chen, C. C. (2020). An activity-based formulation for Langmuir adsorption isotherm. Adsorption, 26(3), 375-386.

Chen, H., Cong, T. N., Yang, W., Tan, C., Li, Y., & Ding, Y. (2009). Progress in electrical energy storage system: A critical review. Progress in natural science, 19(3), 291312.

Dong Zilong, Wu Zhenshen, Li Mengke, Huang Yajie, Chen Junmin, Li Lixin, ... & Xie Liping. (2023). Research progress on the preparation of lignite-based activated carbon. Clean Coal Technology , 29 (2).

Fan, K., Lei, X., Zhang, J., Yu, T., Chen, H., & Liu, J. (2023). Preparation of carbon electrode material with a large specific surface area and multiscale pore structure from biowaste kochia for symmetrical supercapacitor. Energy Technology, 11(4), 2201281.

Feng, H., Zhou, T., Ge, L., Li, Q., Zhao, C., Huang, J., & Wang, Y. (2024). Study on the preparation of high value-added activated carbon from petroleum coke: Comparison between one-and two-step methods for carbonization and activation. Energy, 130570.

Feng, P., Li, J., Wang, H., & Xu, Z. (2020). Biomass-based activated carbon and activators: preparation of activated carbon from corncob by chemical activation with biomass pyrolysis liquids. ACS omega, 5(37), 24064-24072.

Frackowiak, E. (2007). Carbon materials for supercapacitor application. Physical chemistry chemical physics, 9(15), 1774-1785.

Gopalakrishnan, A., & Badhulika, S. (2020). Effect of self-doped heteroatoms on the performance of biomass-derived carbon for supercapacitor applications. Journal of power sources, 480, 228830.

Hasdi, N. D., Ahmad, N., Ahya, M. K., & Puasa, S. W. (2023). An overview of activated carbon preparation from various precursors. Scientific Research Journal, 20(1), 51-87.

Henrietta, H. M., Kalaiyarasi, K., & Raj, A. S. (2022). Coconut tree (Cocos nucifera) products: A review of global cultivation and its benefits. Journal of Sustainability and Environmental Management, 1(2), 257-264.

Hu, Z., & Srinivasan, M. P. (1999). Preparation of high-surface-area activated carbons from coconut shell. Microporous and Mesoporous Materials, 27(1), 11-18.

Ioannidou, O., & Zabaniotou, A. (2007). Agricultural residues as precursors for activated carbon production—A review. Renewable and sustainable energy reviews, 11(9), 1966-2005.

Ismail, A. A., van de Voort, F. R., & Sedman, J. (1997). Fourier transform infrared spectroscopy: principles and applications. In Techniques and instrumentation in analytical chemistry, 18(C), 93–139.

Biomass-derived carbon electrodes for supercapacitors and hybrid solar cells: towards sustainable photo-supercapacitors. Sustainable Energy & Fuels, 5(19), 4784-4806.

Kuperman, A., Aharon, I., Malki, S., & Kara, A. (2012). Design of a semiactive battery-ultracapacitor hybrid energy source. IEEE Transactions on Power Electronics, 28(2), 806-815.

Lee, K. C., Lim, M. S. W., Hong, Z. Y., Chong, S., Tiong, T. J., Pan, G. T., & Huang, C. M. (2021). Coconut shell-derived activated carbon for high-performance solid-state supercapacitors. Energies, 14(15), 4546.

Marpaung, F., Kim, M., Khan, J. H., Konstantinov, K., Yamauchi, Y., Hossain, M. S. A., ... & Kim, J. (2019). Metal–organic framework (MOF)-derived nanoporous carbon materials. Chemistry–An Asian Journal, 14(9), 1331-1343.

Mazlan, M. A. F., Uemura, Y., Yusup, S., Elhassan, F., Uddin, A., Hiwada, A., & Demiya, M. (2016). Activated carbon from rubber wood sawdust by carbon dioxide activation. Procedia engineering, 148, 530-537.

Muttil, N., Jagadeesan, S., Chanda, A., Duke, M., & Singh, S. K. (2022). Production, types, and applications of activated carbon derived from waste tyres: an overview. Applied Sciences, 13(1), 257.

Naji, S. Z., & Tye, C. T. (2022). A review of the synthesis of activated carbon for biodiesel production: Precursor, preparation, and modification. Energy Conversion and Management: X, 13, 100152.

Nor, N. M., Lau, L. C., Lee, K. T., & Mohamed, A. R. (2013). Synthesis of activated carbon from lignocellulosic biomass and its applications in air pollution control—a review. Journal of Environmental Chemical Engineering, 1(4), 658-666.

Nunes, C. A., & Guerreiro, M. C. (2011). Estimation of surface area and pore volume of activated carbons by methylene blue and iodine numbers. Química Nova, 34, 472-476.

Obidoa, O., Joshua, P. E., & Eze, N. J. (2010). Phytochemical analysis of Cocos nucifera L. Journal of Pharmacy Research, 3(2), 280-286.

Pallarés, J., González-Cencerrado, A., & Arauzo, I. (2018). Production and characterization of activated carbon from barley straw by physical activation with carbon dioxide and steam. Biomass and bioenergy, 115, 64-73.

Pintor, M. J., Jean-Marius, C., Jeanne-Rose, V., Taberna, P. L., Simon, P., Gamby, J., ... & Gaspard, S. (2013). Preparation of activated carbon from Turbinaria turbinata seaweeds and its use as supercapacitor electrode materials. Comptes Rendus. Chimie, 16(1), 73-79.

Plaza, M. G., Pevida, C., Martín, C. F., Fermoso, J., Pis, J. J., & Rubiera, F. (2010). Developing almond shell-derived activated carbons as CO2 adsorbents. Separation and Purification Technology, 71(1), 102-106.

Raposo Bejines, F., Rubia, M., & Borja Padilla, R. (2009). Methylene blue number as useful indicator to evaluate the adsorptive capacity of granular activated carbon in batch mode: Influence of adsorbate/adsorbent mass ratio and particle size. Journal of Hazardous Materials, 165(1–3).

Ren, Z., Lan, Y., & Wang, Y. (2013). Aligned carbon nanotubes: physics, concepts, fabrication and devices. NanoScience and Technology, 5.

Şahin, M. E., Blaabjerg, F., & Sangwongwanich, A. (2022). A comprehensive review on supercapacitor applications and developments. Energies, 15(3), 674.

Saratale, R. G., Sivapathan, S. S., J. Jung, W., Kim, H. Y., Saratale, G. D., & Kim, D. S. (2016). Preparation of activated carbons from peach stone by H4P2O7 activation and its application for the removal of Acid Red 18 and dye containing wastewater. Journal of Environmental Science and Health, Part A, 51(2), 164-177.

Shafeeyan, M. S., Daud, W. M. A. W., Houshmand, A., & Shamiri, A. (2010). A review on surface modification of activated carbon for carbon dioxide adsorption. Journal of Analytical and Applied Pyrolysis, 89(2), 143-151.

Shrestha, D., Gyawali, G., & Rajbhandari, A. (2018). Preparation and characterization of activated carbon from waste sawdust from saw mill. Journal of Institute of Science and Technology, 22(2), 103-108.

Shrestha, D., Maensiri, S., Wongpratat, U., Lee, S. W., & Nyachhyon, A. R. (2019). Shorea robusta derived activated carbon decorated with manganese dioxide hybrid composite for improved capacitive behaviors. Journal of Environmental Chemical Engineering, 7(5), 103227.

Shrestha, L. K., Shrestha, R. G., Chaudhary, R., Pradhananga, R. R., Tamrakar, B. M., Shrestha, T., ... & Ariga, K. (2021). Nelumbo nucifera seed–derived nitrogen-doped hierarchically porous carbons as electrode materials for high-performance supercapacitors. Nanomaterials, 11(12), 3175.

Shrestha, S., Dhami, A. K., & Nyachhyon, A. R. (2021). Adsorptive removal of Fe (II) By NaOH treated rice husk: adsorption equilibrium and kinetics. Scientific World, 14(14), 75-82.

Singla, M. K., Gupta, J., Safaraliev, M., Nijhawan, P., Oberoi, A. S., & Menaem, A. A. (2024). Characterization of an activated carbon electrode made from coconut shell precursor for hydrogen storage applications. International Journal of Hydrogen Energy, 61, 1417-1428.

Sriprom, P., Krusong, W., & Assawasaengrat, P. (2021). Preparation of activated carbon from durian rind with difference activations and its optimization. Journal of Renewable Materials, 9(2), 311-324.

Sujiono, E. H., Zabrian, D., Zharvan, V., & Humairah, N. A. (2022). Fabrication and characterization of coconut shell activated carbon using variation chemical activation for wastewater treatment application. Results in Chemistry, 4, 100291.

Taer, E., Agustino, A., Gultom, E. S., & Taslim, R. (2023). Sustainable development of biomass-derived activated carbon through chemical and physical activations

and its effect on the physicochemical and electrochemical activity. Energy Sources, Part A: Recovery, Utilization, and Environmental Effects, 45(1), 319-330.

Titirici, M. M., White, R. J., Brun, N., Budarin, V. L., Su, D. S., Del Monte, F., ... & MacLachlan, M. J. (2015). Sustainable carbon materials. Chemical Society Reviews, 44(1), 250-290.

Wang, Y., Duan, Y., Liang, X., Tang, L., Sun, L., Wang, R., ... & Hu, H. (2023). Hierarchical Porous Activated Carbon Derived from Coconut Shell for Ultrahigh-Performance Supercapacitors. Molecules, 28(20), 7187.

Wasterlain, S., Guven, A., Gualous, H., Fauvarque, J. F., Gallay, R., BâtF, U. T. B. M., & Paris, L. C. (2006). Hybrid power source with batteries and supercapacitor for vehicle applications. Proceedings of the ESCAP, 6.

Wong, S., Ngadi, N., Inuwa, I. M., & Hassan, O. (2018). Recent advances in applications of activated carbon from biowaste for wastewater treatment: a short review. Journal of Cleaner Production, 175, 361-375.

Yahya, M. A., Al-Qodah, Z., & Ngah, C. Z. (2015). Agricultural bio-waste materials as potential sustainable precursors used for activated carbon production: A review. Renewable and sustainable energy reviews, 46, 218-235.

Yahya, M. A., Mansor, M. H., Zolkarnaini, W. A. A. W., Rusli, N. S., Aminuddin, A., Mohamad, K., ... & Ozair, L. N. (2018). A brief review on activated carbon derived from agriculture by-product. In AIP conference proceedings, 1972(1).

Yang, J., & Qiu, K. (2010). Preparation of activated carbons from walnut shells via vacuum chemical activation and their application for methylene blue removal. Chemical Engineering Journal, 165(1), 209-217.

Yorgun, S., Yıldız, D., & Şimşek, Y. E. (2016). Activated carbon from paulownia wood: Yields of chemical activation stages. Energy Sources, Part A: Recovery, Utilization, and Environmental Effects, 38(14), 2035-2042.

Zhang, L. L., & Zhao, X. S. (2009). Carbon-based materials as supercapacitor electrodes. Chemical society reviews, 38(9), 2520-2531.

Zhou, Y., Li, J., Hu, S., Qian, G., Shi, J., Zhao, S., ... & Lian, J. (2022). Sawdust-derived activated carbon with hierarchical pores for high-performance symmetric supercapacitors. Nanomaterials, 12(5), 810.

Preparation and characterization of coconut she...

By: Sarmila Dangi

As of: May 5, 2024 2:48:20 PM
13,954 words - 34 matches - 5 sources

Similarity Index
4%

Mode: Summary Report

Sources:

104 words / 1% - from 02-Feb-2024 12:00AM
elibrary.tucl.edu.np

101 words / 1% - from 02-Feb-2024 12:00AM
elibrary.tucl.edu.np

100 words / 1% - from 02-Feb-2024 12:00AM
elibrary.tucl.edu.np

121 words / 1% - Internet from 21-Jan-2022 12:00AM
nepjol.info

91 words / 1% - Crossref
Samah Zaki Naji, Ching Thian Tye. "A Review of The Synthesis of Activated Carbon For Biodiesel Production: Precursor, Preparation, and Modification", Energy Conversion and Management: X, 2021

Paper text:

PREPARATION AND CHARACTERIZATION OF COCONUT SHELL DERIVED ACTIVATED CARBON FOR SUPERCAPACITOR APPLICATION A DISSERTATION

SUBMITTED TO THE DEPARTMENT OF CHEMISTRY AMRIT CAMPUS INSTITUTE OF SCIENCE AND TECHNOLOGY TRIBHUVAN UNIVERSITY NEPAL FOR THE **PARTIAL FULFILLMENT** OF REQUIREMENT OF **THE** MASTER **OF SCIENCE DEGREE IN CHEMISTRY BY**

SARMILA DANGI SYMBOL NO: 2180/077 T. U. REGD. NO.: 5-2-214-34-2016 MAY, 2024 CHAPTER-1 INTRODUCTION 1.1 General Introduction Carbon-based materials particularly in their activated form, are commonly employed in various aspects of environmental analyses, like purification and pollution remediation, renewable energy generation and storage mechanisms (Titirici et al., 2015). The examples of energy storage are supercapacitors, solar cells, batteries and sensors as well. These materials, including powders, fibers, composites, monoliths, and foils, are distinguished by their high specific surface area, considerable pore volume, mechanical stability, and chemical inertness (Frackowiak, 2007). The term